Award Number:
W81XWH-12-1-0395

TITLE:
A Novel Mechanism for the Pathogenesis of Nonmelanoma Skin Cancer Resulting from Early Exposure to Ultraviolet Light

PRINCIPAL INVESTIGATOR:
Rebecca Morris, PhD

CONTRACTING ORGANIZATION:
University of Minnesota, Twin Cities
Minneapolis, MN 55455-2070

REPORT DATE:
November 2015

TYPE OF REPORT:
Final

PREPARED FOR: U.S. Army Medical Research and Materiel Command
Fort Detrick, Maryland 21702-5012

DISTRIBUTION STATEMENT:

× Approved for public release; distribution unlimited

REPORT DOCUMENTATION PAGE

Form Approved
OMB No. 0704-0188

1. REPORT DATE *(DD-MM-YYYY)*	**2. REPORT TYPE**	**3. DATES COVERED** *(From - To)*
November 2015	Final	1Sep2012 - 31Aug2015

4. TITLE AND SUBTITLE
A Novel Mechanism for the Pathogenesis of Nonmelanoma Skin Cancer Resulting from Early Exposure to Ultraviolet Light

5a. CONTRACT NUMBER

5b. GRANT NUMBER
W81XWY-12-1-0395

5c. PROGRAM ELEMENT NUMBER

6. AUTHOR(S)
Rebecca Morris

E-Mail: rmorris@hi.umn.edu

5d. PROJECT NUMBER

5e. TASK NUMBER

5f. WORK UNIT NUMBER

7. PERFORMING ORGANIZATION NAME(S) AND ADDRESS(ES)

University of Minnesota
Office of Sponsored Projects
200 Oak St. SE
Minneapolis, MN 55455-2009

8. PERFORMING ORGANIZATION REPORT NUMBER

9. SPONSORING / MONITORING AGENCY NAME(S) AND ADDRESS(ES)

U.S. Army Medical Research and
Fort Detrick, Maryland 21702-5012

10. SPONSOR/MONITOR'S ACRONYM(S)

11. SPONSOR/MONITOR'S REPORT NUMBER(S)

12. DISTRIBUTION / AVAILABILITY STATEMENT

Approved for Public Release; Distribution Unlimited

13. SUPPLEMENTARY NOTES
None

14. ABSTRACT Skin egress, entering the circulation, and traveling throughout the body may be a characteristic of skin stem cells. We have made several novel findings in this regard: 1) murine epidermal keratinocytes migrate preferentially in vitro to bone marrow cells, 2) keratinocytes migrate towards SDF1 alpha and HMGB1 baits over control attractants. 3) CD184 is expressed on approximately 27 percent of CD49f+/CD34+ hair follicle stem cells, and 4) CD49f+/Keratin 14+ cells in increase in blood and bone marrow following solar UV treatment. 5) Skin grafting studies demonstrated that grafted cells appear in bone marrow. 6) DMBA/TPA studies showed that keratinocytes migrated from the epidermis during the early stages of skin tumor promotion. 7) We demonstrated using our K14mTmG transgenic mice that a low but significant number of K14-expressing cells are found in the bone marrow. These findings support our hypothesis that: 1) skin egress may be a characteristic of skin stem cells in response to damage, and 2) bone marrow may be a long-lived reservoir of sunlight initiated stem cells that can repopulate the skin even years later following damage to the skin.

15. SUBJECT TERMS
non-melanoma skin cancer, epidermal keratinocytes, stem cells, migration

16. SECURITY CLASSIFICATION OF:			**17. LIMITATION OF ABSTRACT**	**18. NUMBER OF PAGES**	**19a. NAME OF RESPONSIBLE PERSON**
a. REPORT	**b. ABSTRACT**	**c. THIS PAGE**			USAMRMC
U	U	U	U U	37	**19b. TELEPHONE NUMBER** *(include area code)*

TABLE OF CONTENTS

INTRODUCTION:

The epidermal layer of the skin is composed largely of cells called keratinocytes. Keratinocytes in the basal layer are organized into subpopulations based on their proliferative nature and include stem cells (relatively rare) and transit amplifying cells (comprise most of the proliferating cells). When a stem cell divides, one daughter usually remains a stem cell while the other daughter gives rise to transit amplifying cells with limited proliferative potential. Upon completion of their divisions, transit amplifying cells undergo an orderly maturation process called terminal differentiation that includes their outward displacement through the suprabasal layers, production of high molecular weight keratins, loss of their nuclei, and formation of an impervious outer structure called the cornified envelope. This process is exceptionally orderly and maintains the normal thickness and cellularity, and the normal functions of the epidermis throughout life. This proposal focuses on the stem cells of the hair follicles because they not only serve as a reservoir of epidermal cells, they also possess remarkable regenerative potential and are known to be able to reconstitute a graft, to heal wounds, and even to give rise to non-melanoma skin cancer (1). Therefore, identification of stem cell behavioral characteristics and responses are critical problems in cutaneous biology. We proposed here the novel concept that skin egress, entering the circulation, and traveling throughout the body may be a new behavior of epidermal stem cells. We proposed that sunburn following exposure to sunlight has the capacity to make skin stem cells migrate. In this Discovery award we challenged the existing paradigm of skin cells in response to damage. We addressed the following question: Do hair follicle stem cells migrate from the skin following sunburn as a consequence of ultraviolet light induced inflammation? Our hypothesis is that sunburn makes the hair follicles stem cells leave the skin and enter the blood circulation, and home to the bone marrow. Therefore, we proposed in this pilot study to test the first axiom: that CD34 positive keratinocyte stem cells have the capacity for extracutaneous migration. We accomplished this with a novel application of standard in vitro assays together with the use of two transgenic mice that are already available including two UV experiments, and a skin grafting experiment. The rationale for the in vitro experiment was that the cellular and molecular players involved may be identified, isolated, and manipulated. The rationale for the in vivo experiments is that the cellular players also may be identified and isolated and explored systemically under their native conditions.

BODY:

In our Discovery proposal, we submitted two Specific Aims to provide evidence whether or not keratinocyte stem cells may leave the skin and migrate to the bone marrow. We have largely accomplished this objective.

NOTE CONCERNING THE REVISED STATEMENT OF WORK 22APR2105:

In this revised statement of work, we have made only one change: deleting the use of the K15EGFP/TOM mice in Specific Aim 1, Task 2 and in Specific Aim 2, Tasks 7 and 8. This was done because the mice did not breed well enough to produce the requisite number of offspring to enable our experiments. The deletion of these mice in the tasks below is denoted by a strikethrough (~~K15EGFP/TOM~~).

MAJOR OBJECTIVES FOR SPECIFIC AIM 1. The first aim was to determine whether keratinocyte stem cells are chemotactic and attracted towards bone marrow and other tissues in culture. **General Approach.** First, we applied a migration co-culture system where whole bone tissue, including hematopoietic and stromal elements were placed as bait beneath keratinocytes including hair follicle stem cells cultivated on a filter. Keratinocytes were attracted to the bait and migrated through the filter and were quantified. Second, we documented the presence of keratin immunoreactive cells in the blood and bone marrow following exposure of mice to solar UV radiation by fluorescence activated cell sorting (FACS), immunofluorescence microscopy, and by quantitative real-time polymerase chain reaction (qPCR).

SPECIFIC RESULTS FOR AIM 1. The figures are listed in order as an appendix section.

Specific Aim 1, Task 1. Epidermal keratinocytes were harvested from individual mice and placed in a BD Biocoat Matrigel Migration Assay performed according to the manufacturer's directions. The assays were conducted in growth factor and serum-free medium. Results of pilot experiments were used to determine the number of wells needed to achieve statistically significant results. The positive control was a metastatic keratinocyte cell line, and the negative controls included keratinocytes cultured on the filters without bone tissue in the chamber, "irrelevant" cells such as 3T3 cells as bait, serum-free medium, examination of filters without cells (as a control on the staining procedure), examination of various cell densities to determine the keratinocyte seeding density most appropriate for studying influences on migration (linear portion of scale) and time courses to determine the most appropriate intervals. Keratinocytes were placed on the dish insert and a) whole crushed bone and b) bone marrow conditioned medium were individually placed in the well. **Figure 1a** demonstrates the results of duplicate experiments indicating that 0.5x10^6 cells per well was an optimal seeding density as we wanted to be on an approximately linear range of the seeding dose-response. **Figure 1b** demonstrates the effect of migration time on the number of migrated keratinocytes. Because the 36-hour time point showed the least variance and the greatest reproducibility among experimental replicates and because it was midway between the shortest and longest timepoints, it was chosen as the timepoint for comparison with test baits. Figures 1a and 1b led up to our test experiment comparing the effects of bone marrow and bone marrow conditioned medium on the migration of epidermal keratinocytes (**Figure 1c**). Several interesting findings emerge from this Figure 1c. First, epidermal keratinocytes are strongly attracted to the bone marrow with its conditioned medium as well as to bone marrow conditioned medium alone. Second, the epidermal keratinocytes are minimally attracted to other controls such as 3T3 cells, or even to DMEM with 10% FBS. A third and potentially interesting finding is that bone marrow cells are rather well attracted to epidermal keratinocytes in DMEM without FBS.

Specific Aim 1, Task 2. In the second in vitro experiment, we performed FACS analysis on mouse skin keratinocytes immunostained with antibodies to alpha-6 integrin (CD49f), CD34, and CXCR4 (the receptor for SDF1). Although there is some indication in the literature that epidermal keratinocytes express this receptor, we wanted to determine specifically which subpopulation of keratinocytes (the CD49f+/CD34+ hair follicle stem cells) expressed this receptor. Keratinocytes were harvested from five individual C57BL/6 female mice and processed for FACS analysis as we have previously reported. Positive controls were bone marrow stromal cells. Negative controls were isotype control antibodies. **Figure 2a** details the FACS sorting of freshly harvested epidermal keratinocytes stained with fluorescent antibodies to CD49f (alpha 6 integrin, the external component of the hemidesmosomes found on all basal keratinocytes), CD34 expressed on hair follicle stem cells, and CD184 (also known as CXCR4, the receptor for stromal derived factor 1 alpha (SDF1 alpha). We note with interest that 10.7% of the CD49+/CD34+ hair follicle stem cells are also positive for CD184. This finding is interesting to us because, the keratinocytes that have the receptor for CXCL12 would be the most likely cells to be able to respond to it. Here we demonstrated that the CD49f+/CD34 double positive hair follicle stem cells are among those cells. In light of our finding a paper reporting that a subset of lineage-/Sca1+ bone marrow progenitors expresses the PDGFR1 alpha (CD140) and is recruited from the bone marrow to grafted skin where they apparently become epithelial cells (Tamai et al., PNAS, 2010), and because we could find no confirmation of this report, we used some of our leftover cells to determine whether we could also find this population. Our attempts proved fruitful as demonstrated in **Figure 2b** (without lineage depletion) and **Figure 2c** (with lineage depletion). This is significant because these bone marrow cells may be the ones that are attracted to the keratinocyte bait shown in **Figure 1c**.

Specific Aim 1, Task 3. Epidermal keratinocytes were harvested from individual ~~K15EGFP~~ K14EGFP/TOM mice will be placed in the Matrigel invasion assay as summarized in Experiment 1. In this experiment we specifically focused on the percentage of the ~~K15EGFP~~ immunoreactive cells. This task was not accomplished in Year 01 because the ~~K15EGFP~~ mice were no longer available. We had hoped to accomplish this task in Year 02 by using FACS-sorted CD49f+/CD34+ hair follicle stem cells (the same cells that express the keratin 15 marker); however the results were not very informative and the experiments will have to be repeated.

Specific Aim 1, Task 4. In this in vitro experiment, keratinocytes were harvested from individual mice. Keratinocytes were placed on the Matrigel filters, and stromal derived factor-1 was placed in the wells at concentrations of 400 to 800 ng/ml as bait. Positive and negative controls, and analyses were performed a summarized in Experiment 1. **Figure 3a** illustrates that freshly harvested epidermal keratinocytes are attracted to 800 ng/ml of SDF1 alpha (CXCL12) more than they are attracted to 3T3 or DMEM without serum, but almost as much as to DMEM with 10% FBS. We await quantification of our second and third experiments. **Figure 3b** shows our first attempt to assess keratinocyte and bone marrow migration toward HMGB1 bait (HMGB1 is the ligand for the PDGFR1 alpha). We believe that there were problems with the keratinocytes in this determination as the controls were so low. A second determination is illustrated in **Figure 3c** where the controls are as expected. This figure demonstrates that, although epidermal keratinocytes appear not to be attracted to mouse HMGB1 protein above the controls, the bone marrow cells are strongly attracted to it. This observation is consistent with that of **Figure 1c** showing that a subset of lineage depleted bone marrow cells indeed has the PDGFR1 alpha, the receptor for HMGB1.

MAJOR MILESTONES FOR SPECIFIC AIM 1. We found that keratinocyte stem cells migrate through the filters towards the bone marrow as compared with requisite positive and negative controls. We also found a significant increase in the number of CD49f+/Keratin 14+ cells in blood and bone marrow following exposure of the mice to solar UV radiation long before the anticipated development of skin tumors relevant to Aim 2, Task 5.

MAJOR OBJECTIVES FOR AIM 2 The focus of this in vivo aim was to determine whether hair follicle stem cells or their progeny migrate from the skin during ultraviolet light induced inflammation and carcinogenesis. **General Approach.** We established skin grafts of Krt1-14EGFP/TOM enriched and depleted subpopulations, and quantified by FACS, fluorescent keratinocytes in the dermis, blood, bone marrow and other tissues.

MAJOR TASKS FOR AIM 2

Specific Aim 2, Task 5. In experiment 2, we exposed mice to artificial sunlight. At the intervals following exposure to artificial sunlight, groups of 2 mice of each genotype were euthanized, and "green" EGFP-reactive cells in the epidermis and hair follicles, dermis, blood, lymph nodes, and bone marrow will quantified by light microscopy. Typically, 1000 to 5000 cells are counted.

RESULTS RELEVANT TO SPECIFC AIM 2, TASK 5

In preparation for Specific Aim 2, Task 5 to be conducted during Year 02, we examined keratinocytes, blood, and bone marrow by FACS to determine whether we could detect keratin 14 immunoreactivity in blood and bone marrow. As illustrated in **Figure 4a**, the percentage of keratin 14 expressing cells is normally quite low in both blood and bone marrow, but increases considerably in response to solar UV treatment. At the moment, we do not yet know whether this UV-dependent increase is a consequence of keratinocyte egress from the skin; however, we also had the opportunity to obtain bone marrow from euthanized mice in ongoing tumor experiments from other investigators at the Hormel Institute, and we looked for keratin 14 immunoreactive cells in blood and bone marrow by light microscopy of smears of nucleated cells. Although we still need more experience to perfect this experimental method, we were able to confirm the presence of keratin 14 immunoreactive cells in both blood and bone marrow as summarized in the table labeled **Figure 4b**. To investigative further this novel observation, we performed qPCR on freshly harvested epidermal keratinocytes, and on mononuclear cells from blood and bone marrow. As expected, both keratins 14 and 15 were detected in epidermal keratinocytes (Fig**ure 4c**). However, we also detected them in blood and bone marrow from C57BL/6 mice, and keratin 14 only in the blood and bone marrow of BALB/c mice (**Figure 4c**). Therefore, we have confirmed the presence of epidermal cytokeratin 14 by three different methods, by FACS, by immunofluorescence microscopy, and by qPCR. Additionally, we demonstrate in **Figure 5** the use of

genetically defined cytokeratin 14 in the K14EGFP/TOM mouse to quantify the "green" K14-expressing cells. Additional statistical support for this experiment was provided by our mathematician colleague, Derek Gordon. Dr. Gordon (Department of Genetics; Rutgers University). An initial draft of his analysis is provided in the **Other Support** section of this report.

Specific Aim 2, Task 6. In this experiment epidermal keratinocytes were harvested from K14EGFP/TOM ~~K15EGFP~~ female mice and from wild-type littermates. For the skin reconstitution assay, keratinocytes were surgically implanted onto a 1 cm diameter area of dorsal fascia using a silicone chamber initially to contain the cells. The grafts will be placed on SCID female mice. These grafts completely stabilized 1 to 2 weeks following implantation. All surgical procedures were conducted on anesthetized mice in a laminar flow hood with sterile technique according to procedures of the University of Minnesota Research Animal Resources. Groups of 5 grafts will be harvested at 4 day, 7 day, and 14 day time points. "Green" EGFP reactive keratinocytes were quantified by fluorescence microscopy or EGFP immunostaining in the grafts as well as in dermis, blood, lymph nodes and bone marrow as described under Specific Aim 1, above. Two Tables **(Tables 1, and 2)** document our raw data; however, further summary and analysis is ongoing at the present time.

MAJOR MILESTONES ANTICIPATED FOR AIM 2. In the first experiment (Task 5), if our hypothesis is correct, then we would expect to see a UV dose-dependent increase in the number of skin-derived EGFP-reactive keratinocytes in non-cutaneous tissues. If our hypothesis is partially correct, we should find metastatic cells during the later stages of skin tumor progression. Similarly, in the second experiment, we would find EGFP immunoreactive keratinocytes in non-cutaneous tissues following establishment of the skin grafts. Either positive or negative results in either of these experiments would be significant and would be worth accomplishing.

NOTE CONCERNING THE REVISED STATEMENT OF WORK 10APR2014:

We made four changes to our originally proposed Statement of Work. The first three changes involved mouse strains only and no change in the experimental procedures. The fourth change involved a procedure where we add a better-characterized and more-timely model to Specific Aim 2.
First, we substituted ~~K15EGFP/TOM~~ female mice (bred from K15CrePR1 x ROSAmTomato/mEGFP reporter mice) for the K15EGFP mice that are no longer available (the K15EGFP strain was frozen down in the time between submission of our proposal and its award). Second, we added K14EGFP/TOM mice (bred from K14Cre x ROSAmTomato/mEGFP reporter mice) as a control for the ~~K15EGFP/TO~~M mice because this K15 promoter is known to be leaky, and because the K14Cre mouse should label robustly all proliferating epidermal basal cells rather than the progeny of the K15-expressing hair follicle stem cells alone. Third, we added an additional 12 UBC/EGFP mice as "green-only" controls for our originally proposed FACS experiments because we had not proposed sufficient "green-only" controls for these experiments. Lastly, we proposed two DMBA/TPA experiments to supplement the UV experiment in Specific Aim 2 (new Tasks 7 and 8) because we realized that we could obtain a definitive and more timely answer to our question with this well-characterized chemical model of skin carcinogenesis than with the UV carcinogenesis model the early stages of which needed additional characterization which is outside the scope of this project.

We note that even though our K14EGFP/TOM experiments are behind schedule due to the poor breeding of these mice, we expect to be able to finish all experiments with the K14EGFP/TOM mice as planned in the coming unfunded year; however, we do not expect to be able to complete the experiments with the ~~K15EGFP/TOM~~ mice proposed in the revised SOW due to poor breeding of the mice and lack of funds.

Changes to our originally proposed Statement of Work below are given in italics.

MAJOR TASKS FOR SPECIFIC AIM 2

Specific Aim 2, Task 5 (20 female *K14EGFP/TOM* and 20 wild-type littermates). In preparation for Specific Aim 2, Task 5 we examined in Year 01 keratinocytes, blood, and bone marrow by FACS to determine whether

we could detect keratin 14 immunoreactivity in blood and bone marrow. We had demonstrated that the percentage of keratin 14 expressing cells is normally quite low in both blood and bone marrow, but increases considerably in response to solar UV treatment. We still do not yet know whether this UV-dependent increase is a consequence of keratinocyte egress from the skin; however, we also had the opportunity to obtain bone marrow from euthanized mice in ongoing tumor experiments from other investigators at the Hormel Institute, and we looked for keratin 14 immunoreactive cells in blood and bone marrow by light microscopy of smears of nucleated cells. Although we still need more experience to perfect this experimental method, we were able to confirm the presence of keratin 14 immunoreactive cells in both blood and bone marrow. To investigate further this novel observation, we performed qPCR on freshly harvested epidermal keratinocytes, and on mononuclear cells from blood and bone marrow. As expected, both keratins 14 and 15 were detected in epidermal keratinocytes. However, we also detected them in blood and bone marrow from C57BL/6 mice and keratin 14 only in the blood and bone marrow of BALB/c mice. Therefore, we have confirmed the presence of epidermal cytokeratin 14 by three different methods, by FACS, by immunofluorescence microscopy, and by qPCR. In Year 02, we confirmed these results and extended them with our K14EGFP/TOM mice. We found that by using this transgenic model, there were green EGFP fluorescent cells present in blood and bone marrow. This is a highly significant and exciting finding because the transgenic model did not depend upon immunostaining or qPCR. **Figure 5** demonstrates that the number of "green" cells in the bone marrow of K14EGFP/TOM (hybrid) mice increases as the number of counted cells increases.

Specific Aim 2, Task 6 (15 female *K14EGFP/TOM* mice and 15 female wild-type littermates, 30 female SCID mice). In this experiment epidermal keratinocytes were harvested from *K14EGFP/TOM* female mice and from wild-type littermates. For the skin reconstitution assay, keratinocytes were surgically implanted onto a 1 cm diameter area of dorsal fascia using a silicone chamber initially to contain the cells. The grafts were replaced on SCID female mice. These grafts stabilized 1 week following implantation. All surgical procedures were conducted on anesthetized mice in a laminar flow hood with sterile technique according to procedures of the University of Minnesota Research Animal Resources. Groups of 5 grafts were harvested at 4 day, 7 day, and 14 day time points. "Green" EGFP fluorescent keratinocytes were quantified by FACS in blood and bone marrow. In the grafts, we observed a small amount of epithelial tissue that had formed by 7 days post-surgery, and robust engraftment of epithelial tissue at 14 days. Immunohistochemistry has not yet been performed on the grafts themselves. In summary, we did not find EGFP fluorescent cells in bone marrow from any of the SCID mice. Some green cells were seen in blood from both SCID mice that received the CRE-negative control cells. Some green cells were observed in blood of SCID mice receiving hybrid cells. We cannot accurately interpret the results from this experiment due to a "tail-like" artifact in our FACS plots that we believe might be due to cells damaged in the lysing process to remove red blood cells.

Specific Aim 2, Task 7 (5 female K14EGFP/TOM mice and 5 female wild-type littermates, 5 female C57BL/6). *In this experiment, K14EGFP/TOM, wild-type littermates, and B6 mice received one dose of DMBA followed by three applications of TPA or acetone weekly for two weeks. After two weeks of TPA promotion, all mice were euthanized. "Green" EGFP reactive keratinocytes were quantified by FACS of blood and bone marrow.* A partial analysis of photomicrographs is summarized in **Figures 6 and 7**. Figures 6 and 7 summarize "green" cells in bone marrow, with Figure 6 being the broad pictures, and Figure 7 zooming in on the low, but reproducible, level of "green" cells in bone marrow in response to DMBA and TPA treatment. Similarly, **Figures 8 and 9** summarize cell counts in blood, with Figures 8 being the broader pictures and Figure 9 zooming in on the low, but reproducible, level of green cells in the blood. Basically, we observed more EGFP positive and EGFP/TOM double positive cells in blood than in bone marrow. Unexpectedly, there were fewer cells in the DMBA/TPA treated group than in the control treated groups (ACE/TPA, DMBA/ACE, and ACE/ACE). The interpretation of this is not readily apparent, and we expect that we will need to investigate the time-course during TPA promotion in greater detail. Nevertheless, we can conclude from this experiment that DMBA/TPA treatment of the skin results in an increase in K14EGFP positive cells in the blood and bone marrow.

Specific Aim 2, Task 8 (4 male K14EGFP/TOM mice, 4 male UBC/GFP mice, 4 male C57BL/6 and 27 female C57BL/6; 4 male K14EGFP/TOM mice, 4 male UBC/GFP, 4 male C57BL/6 and 27 female C57BL/6 mice). *In this experiment, female B6 bone marrow transplant (BMT) recipient mice received bone marrow transplants from male K14EGFP/TOM, UBC/GFP, or B6 mice that had been treated with one dose of DMBA followed by three applications of TPA or acetone weekly for two weeks. After four weeks of BMT engraftment, female BMT recipients received three applications of TPA or acetone weekly for two weeks then all mice were euthanized. "Green" EGFP reactive keratinocytes were quantified by fluorescence microscopy or EGFP immunostaining in the dermis, blood, lymph nodes, and bone marrow as described. Blood and bone marrow samples were analyzed with FACS to determine differences in populations of "green" EGFP expressing cells after different treatments of DMBA/TPA. For FACS analysis, UBC/EGFP control mice are needed to calibrate the flow cytometer.* **Figure 10** shows an increased number of EGFP immunoreactive bone marrow derived cells migrating to the skin relative to controls early in the course of TPA tumor promotion. These data do not demonstrate the return of egressed keratinocyte from bone marrow back to the skin; however, the sample size was too small and an insufficient number of cells was counted.

MAJOR MILESTONES FOR AIM 2. In the first experiment, if our hypotheses were correct, then we would expect to see a UV dose-dependent increase in the number of skin-derived EGFP-reactive keratinocytes in non-cutaneous tissues that we indeed do observe. If our hypotheses were partially correct, we should find metastatic cells during the later stages of skin tumor progression. Similarly, in the second experiment, we would find EGFP immunoreactive keratinocytes in blood and bone marrow following establishment of the skin grafts. The results of our first experiment were equivocal and must be confirmed. Substantial analysis of tissue samples will follow through next year, as the poor breeding of transgenic mice thwarted our efforts for a timely conclusion of this project.

KEY RESEARCH ACCOMPLISHMENTS :

- Freshly harvested murine epidermal keratinocytes migrate preferentially to whole living bone marrow with bone marrow conditioned medium.
- Freshly harvested murine epidermal keratinocytes migrate to SDF1 alpha, while bone marrow cells migrate to HMGB1 better than freshly harvested epidermal keratinocytes.
- CD184 (SDFR1 alpha) is expressed on approximately 27 percent of CD49f+/CD34+ hair follicle stem cells.
- There is an increase in keratin 14 immunoreactive cells in blood and bone marrow of normal (untreated control) mice as well as a possible increase in keratin 14 expression following solar UV treatment to the dorsum of mice as determined by FACS, immunofluorescence microscopy, and quantitative real-time PCR.
- Two skin grafting studies were performed. The second study yielded viable results, the first study having failed due to difficulties in processing blood and bone marrow for FACS.
- We demonstrated using our K14EGFP/TOM transgenic mice that a low, but significant number of K14 expressing cells are found in the bone marrow in response to DMBA/TPA treatment of the skin well before the development of benign skin lesions.

REPORTABLE OUTCOMES:

- Abstracts were submitted to the Annual Meeting of the Society for Investigative Dermatology and to the Gordon Research Conference on Epithelial Differentiation and Keratinization. The abstract for the SID Meeting was published and presented as a talk in April of 2015. A copy of this abstract is included in the Appendix. Abstracts presented at the GRC are never published or distributed. We had expected to make a presentation of this research at the International Skin Carcinogenesis Conference in June of 2014, but had to decline to the death in the P.I.'s family.
- Submission of two Manuscripts are anticipated by the Summer of 2016.

- One additional pilot project was submitted to the Masonic Cancer Center of the University of Minnesota using some of the data from this DOD award to broaden the concepts we developed here. Additionally, we applied for an additional pilot project from the MCC in October 2105 to explore the function of bone marrow epithelial trafficking in skin carcinogenesis. We expect to learn the results of this proposal 04Dec2015.
- Software was written by our mathematician colleague, Derek Gordon (Department of Genetics at Rutgers University; not as part of this grant) for data obtained from Specific Aim 2, Task 5 that ultimately helped us to have more confidence in our data for this project that had low level, but reproducible, FACS counts ("flirting with 0").
- We anticipate submitting an R01 proposal on the subject of this DOD award in February 2016.

CONCLUSIONS FROM OUR RESEARCH:

We conclude that the data presented herein support our novel hypothesis that (mouse) skin keratinocytes can leave the cutaneous epithelium and enter the blood and bone marrow. Our findings suggest that medical implications would be that the bone marrow could be a reservoir of transformed keratinocytes with the potential to migrate back to the skin as cancer initiating cells upon further damage to the skin. The implications for the US Military would be 1) the need to prevent the first damaging exposure to the skin, and 2) the need to prevent the re-recruitment of the initiated keratinocytes back to the skin by manipulating the cytokine pathways used (possibly SDF1alpha or HMGB1?) upon further damage to the skin such as by combat wounds. Further, results presented here and by complementary findings in humans that we will propose in an R01 next year, would suggest that the number of keratin 14-expressing cells in the blood could provide a simple test for persons at risk for developing non-melanoma skin cancer and perhaps other epithelial cancers.

REFERENCES:

1. Li, S., Park, H., Trempus, C.S., Gordon, D., Liu, Y., Cotsarelis, G., and **Morris, R.J.** Keratin 15 expressing stem cells from the hair follicles contribute to papilloma development in the mouse. Mol. Carcinogenesis 2012, Epub ahead of print, Li, Park, and Trempus share equally as first author.

2. Tamai, K., Yamazaki, T., Chino, T., Ishii, M., Otsuru, S., Kikuchi, Y., Iinima, S., Kaga, K., Nimura, K., Shimbo, T., Umegaki, N., Katayama, I., Miyazaki, J., Takeda, J., McGrath, J.A., Uitto, J., and Kaneda, Y. PDGFR1 alpha-positive cells in bone marrow are mobilized by high mobility group box 1 (HMGB1) to regenerate injured epithelia. Proc. Natl. Acad. Sci. USA 108: 6609-6614, 2011.

APPENDIX:

The Figures representing the principal findings follow here in order as one page per figure together with descriptive legends. Twelve (21) pages of Appendix Figures follow.

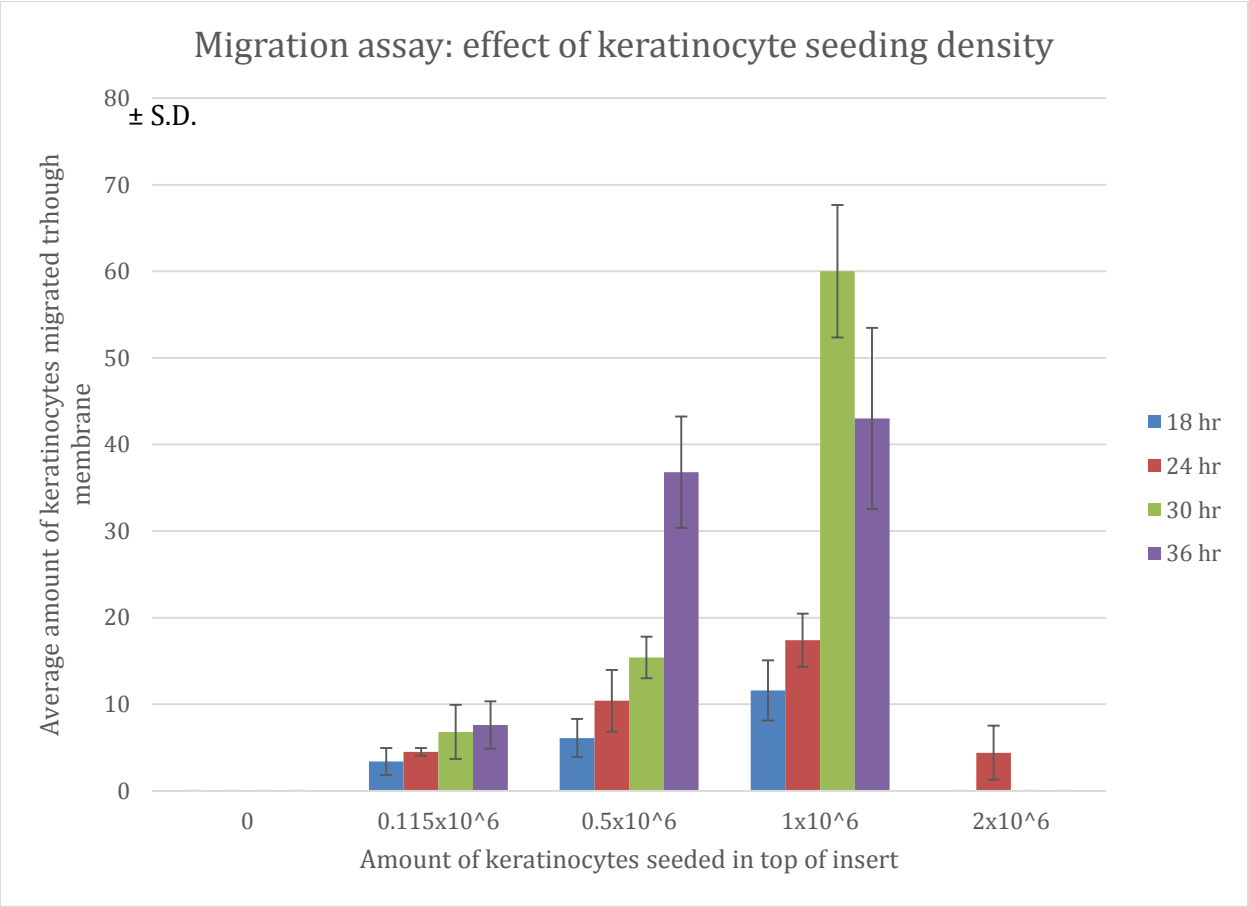

Figure 1a. Keratinocyte dose response Optimal keratinocyte seeding density was determined to be 0.5x10^6 keratinocytes per insert. This chart is a representative assay of 2 performed. Each assay consisted of 3 wells per time point for each condition.

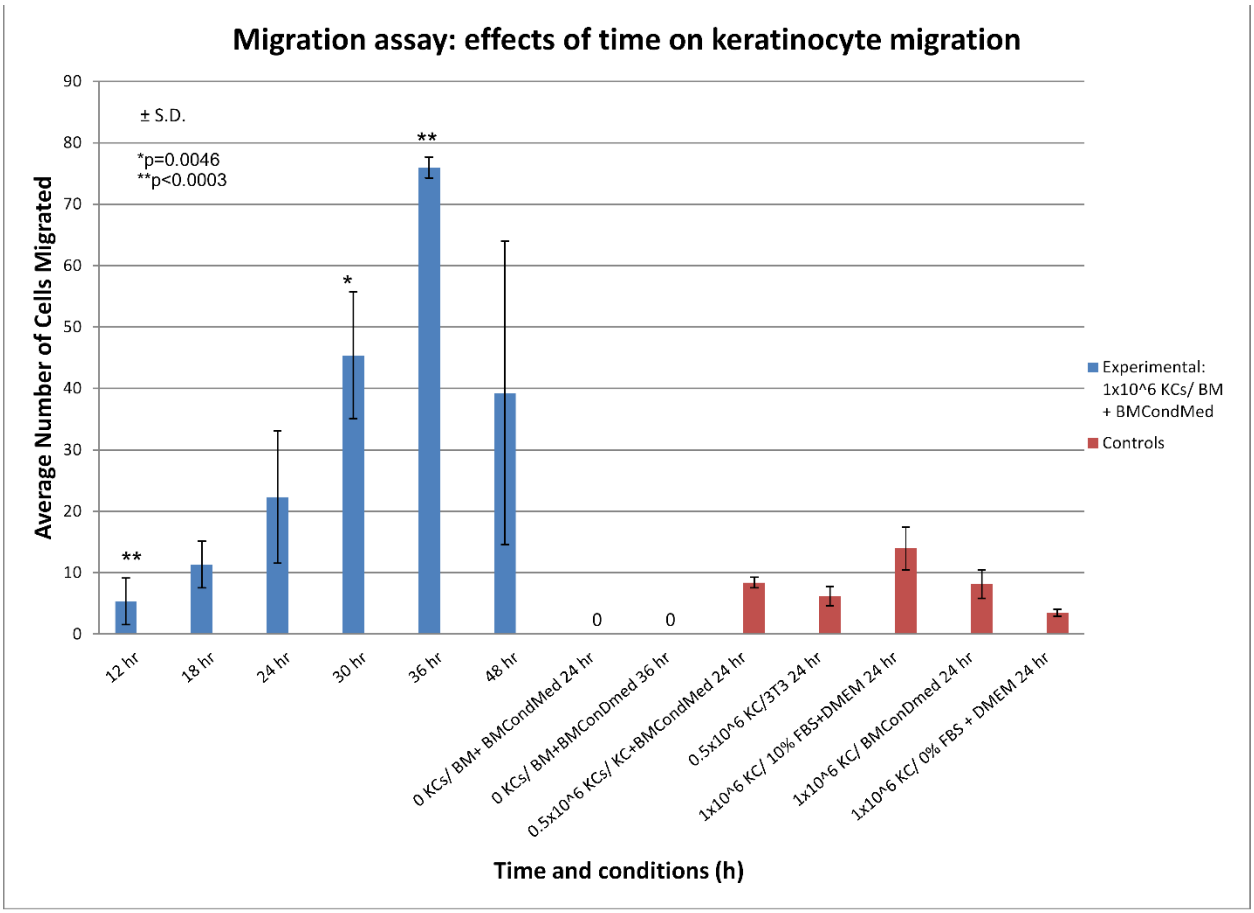

Figure 1b. Keratinocyte time response. This chart shows that the optimal migration time was determined to be 36 hours. This chart is the compiled data of 3 assays performed, each consisting of 3 wells per condition.

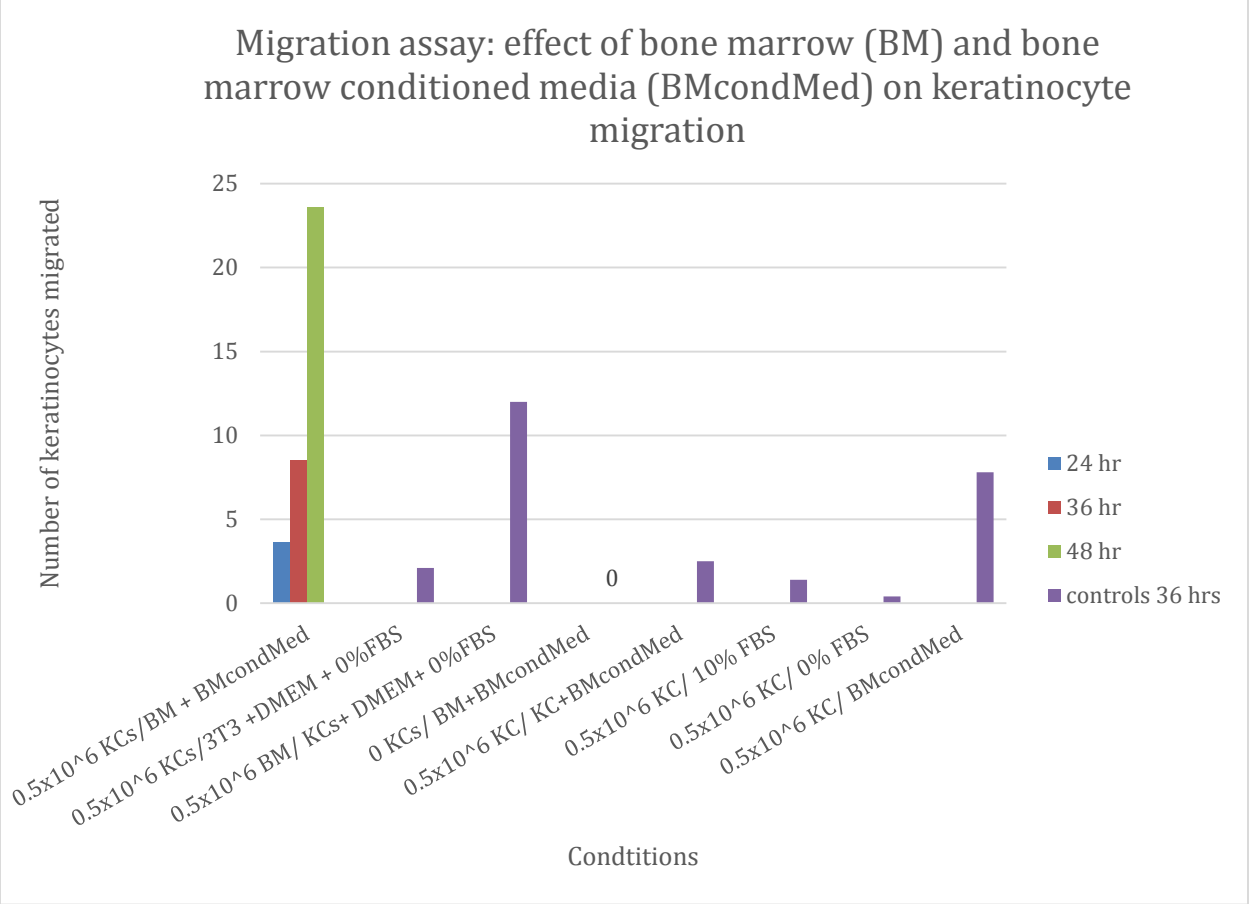

Figure 1c. Keratinocyte Migration with Bone Marrow or Bone Marrow Conditioned Media as chemo-attractant. These data are representative of 2 assays with each assay consisting of 3 wells for each condition except for the experimental well of 0.5x10^6 KCs over BM+BMcondMed at 36 hours which used 6 wells. The point of this figure is that freshly harvester epidermal keratinocytes migrate through Matrigel and a filter towards bait consisting of bone marrow cells and their conditioned medium. These results also demonstrate that bone marrow cells migrate towards epidermal keratinocytes.

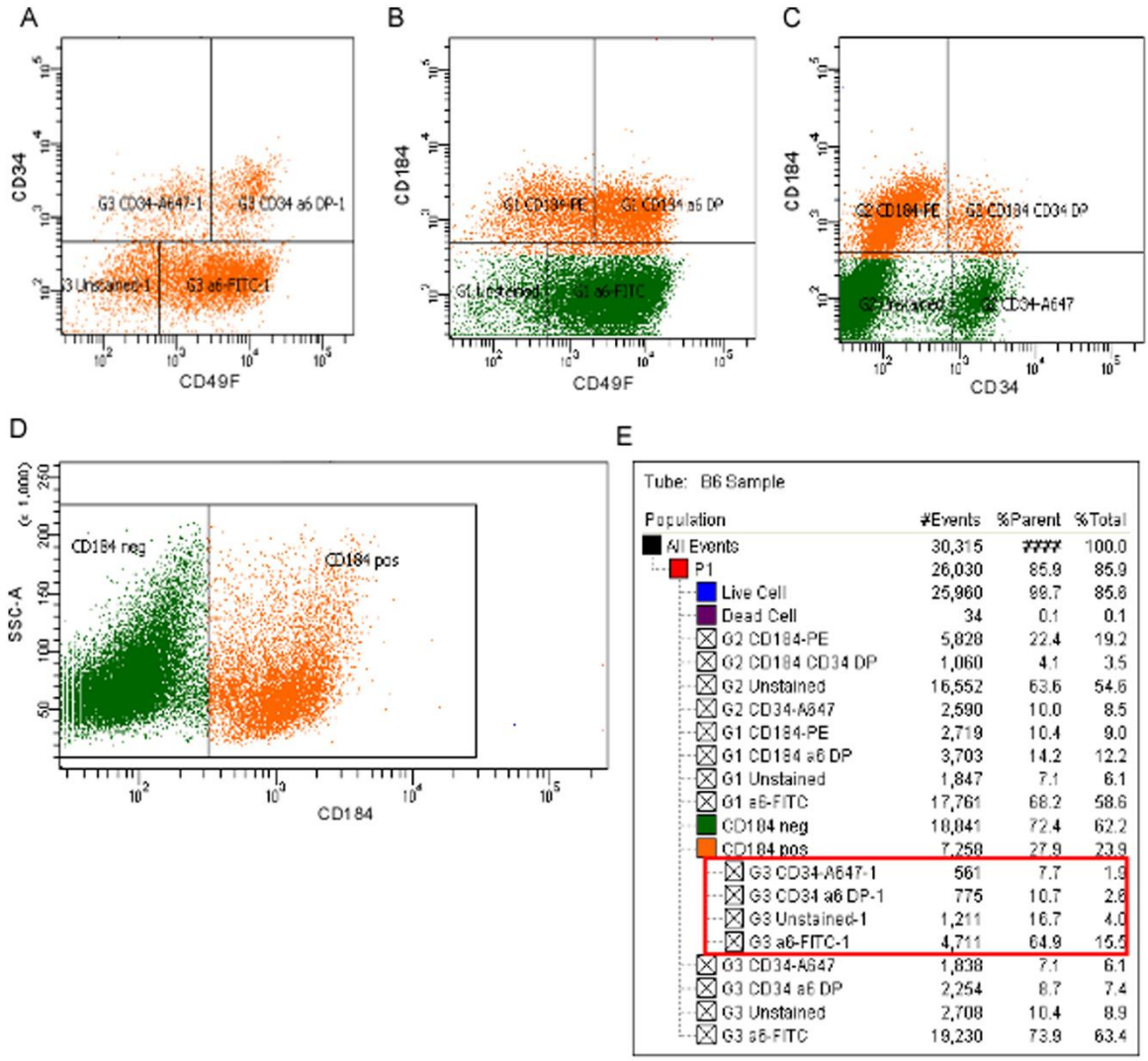

Figure 2a. FACS plot of a6+/CD34+/CXCR4+. FACS report from analysis of CD34, CD49f, and CD184 (Sdf-1 alpha receptor (also known as CXCR4) on freshly harvested murine epidermal keratinocytes.
A: Cells that are CD34+ and CD49f+ (a6+) double positive; 8.7% of the parent population.
B: Cells that are CD184+ (sdf1R+) and CD49f+ (a6+) double positive; 14.2% of the parent population.
C: Cells that are CD184+ (sdf1R+) and CD34+; 4.1% of the parent population.
D: Total count of cells that are positive for CD184+ (sdf1R+); 27.9% of the parent population.
E: Table of the percentages of cells in different gated populations during flow cytometry. Cells that are CD34+, CD49f+ (a6+), and CD184+ (sdf1R+) triple positive account for 10.7% of the parent population.

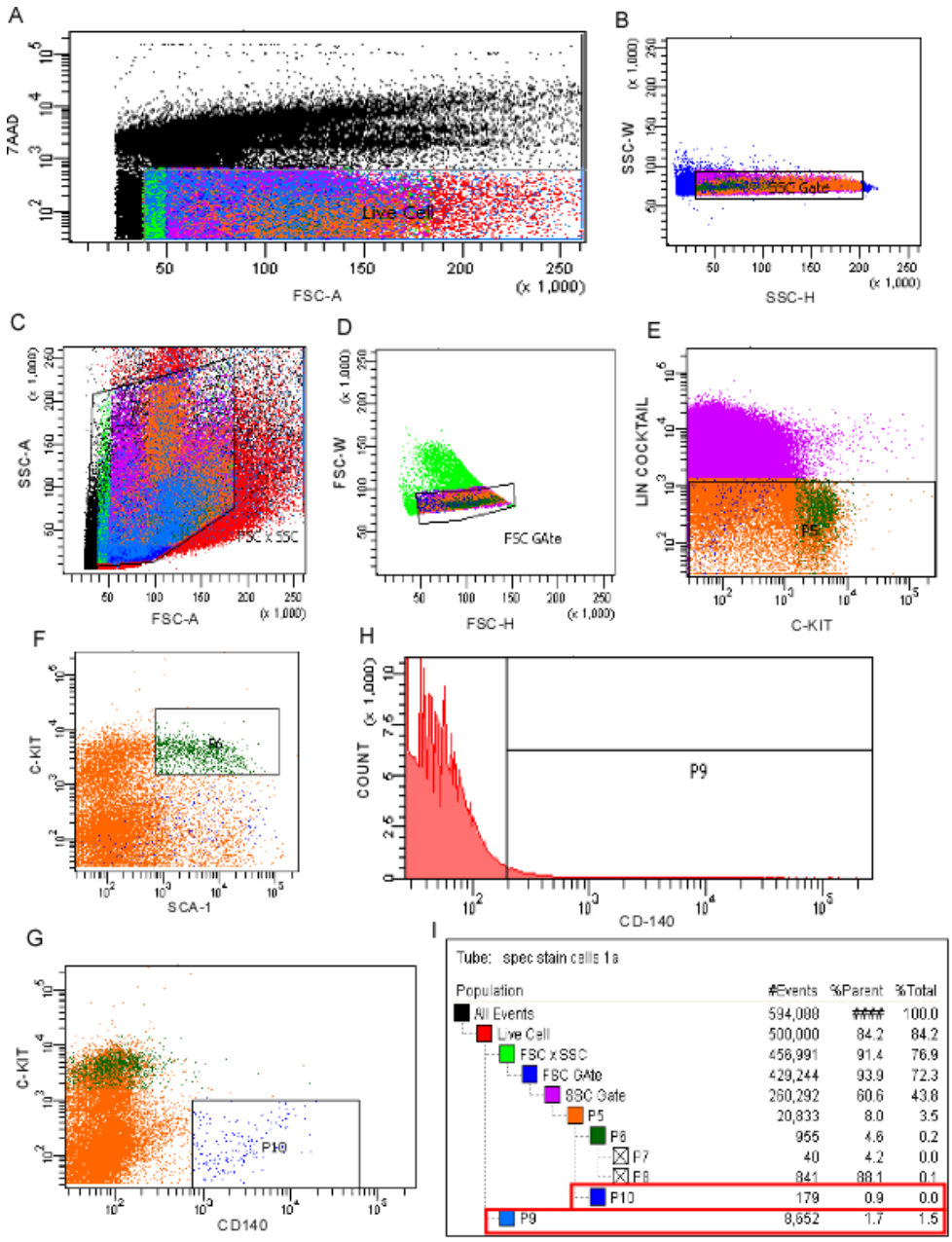

Figure 2b. FACS plot of a6+/CD34+/PDGFRa+, No lineage depletion. FACS analysis on harvested bone marrow cells without lineage depletion using the BD hematopoetic stem cell and progenitor cell kit in conjunction with CD140 (PDGFRa).
A: Gating for live cells of interest.
B-D: Forward and side scatter gating
E: dot plot with P5 representing the population of target hematopoetic stem cells and progenitor cells.
F: P6 is the population of cells that are progenitor cells.
G: P10 represents the population of CD140 positive cells from the progenitor cells.
H: Histogram of progenitor cells with P9 representing the gate for CD140 positive cells of the progenitor cells.
I: Table showing percent of cell populations. P10 shows that 0.9% of the parent population of progenitor cells are CD140 positive. P9 shows that 1.7% of all cells are CD140 positive.

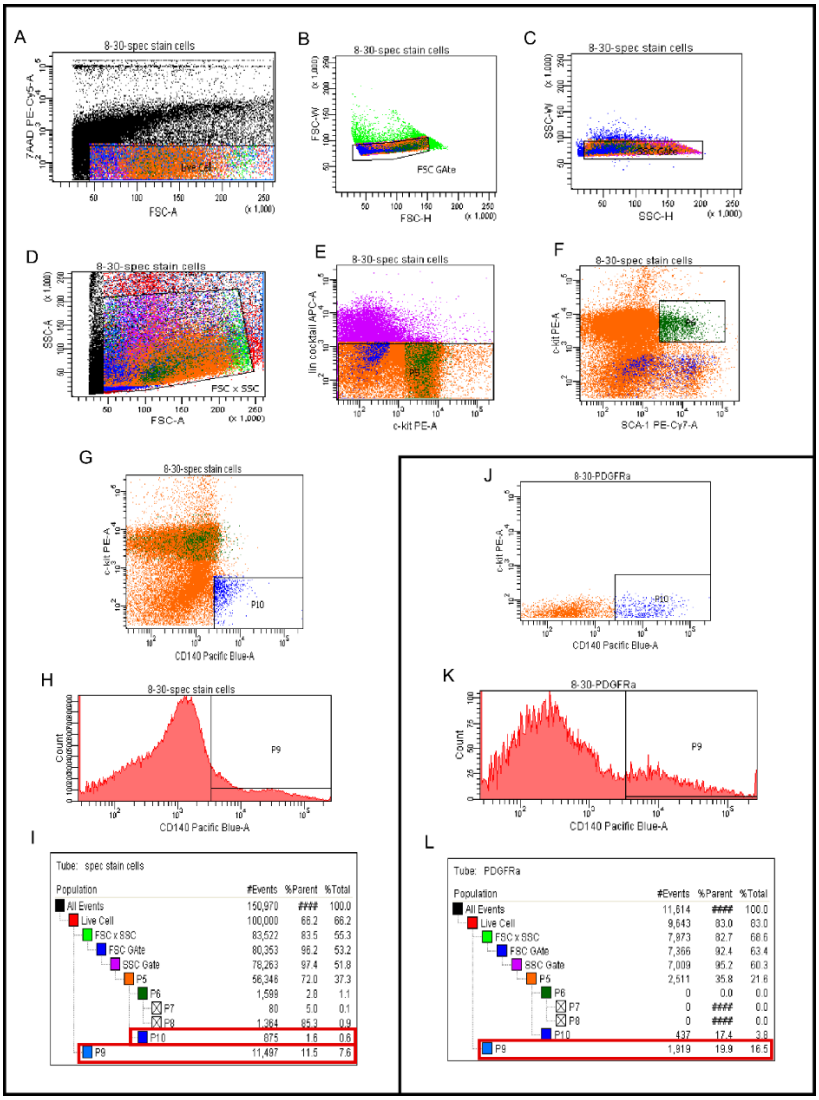

Figure 2c. FACS plot of a6+/CD34+/PDGFRa+, Lineage depletion. FACS analysis on harvested bone marrow cells with lineage depletion using the BD hematopoetic stem cell and progenitor cell kit in conjunction with CD140 (PDGFRa).

A: Live lineage depleted cells.

B-D: Forward and side scatter gating

E: dot plot with P5 representing the population of target progenitor cells.

F: P6 is the population of cells that are lineage depleted progenitor cells. G: P10 represents the population of CD140 positive cells from the lineage depleted progenitor cells.

H: Histogram of CD140 positive cells of the lineage depleted progenitor cells.

I: Table showing percent of cell populations. P10 shows that 1.6% of the parent population of lineage depleted progenitor cells are CD140 positive. P9 shows that 11.5% of all lineage depleted cells are CD140 positive.

J: Resulting dot plot with only CD140 (PDGFRa). The population of lineage depleted cells that are CD140 positive are in gate P10 in blue.

K: The histogram of the dot plot in J showing the population of CD140 positive cells in the P9 region.

L: Table showing percentage of CD140 positive cells is about 20% of the parent population of lineage depleted cells.

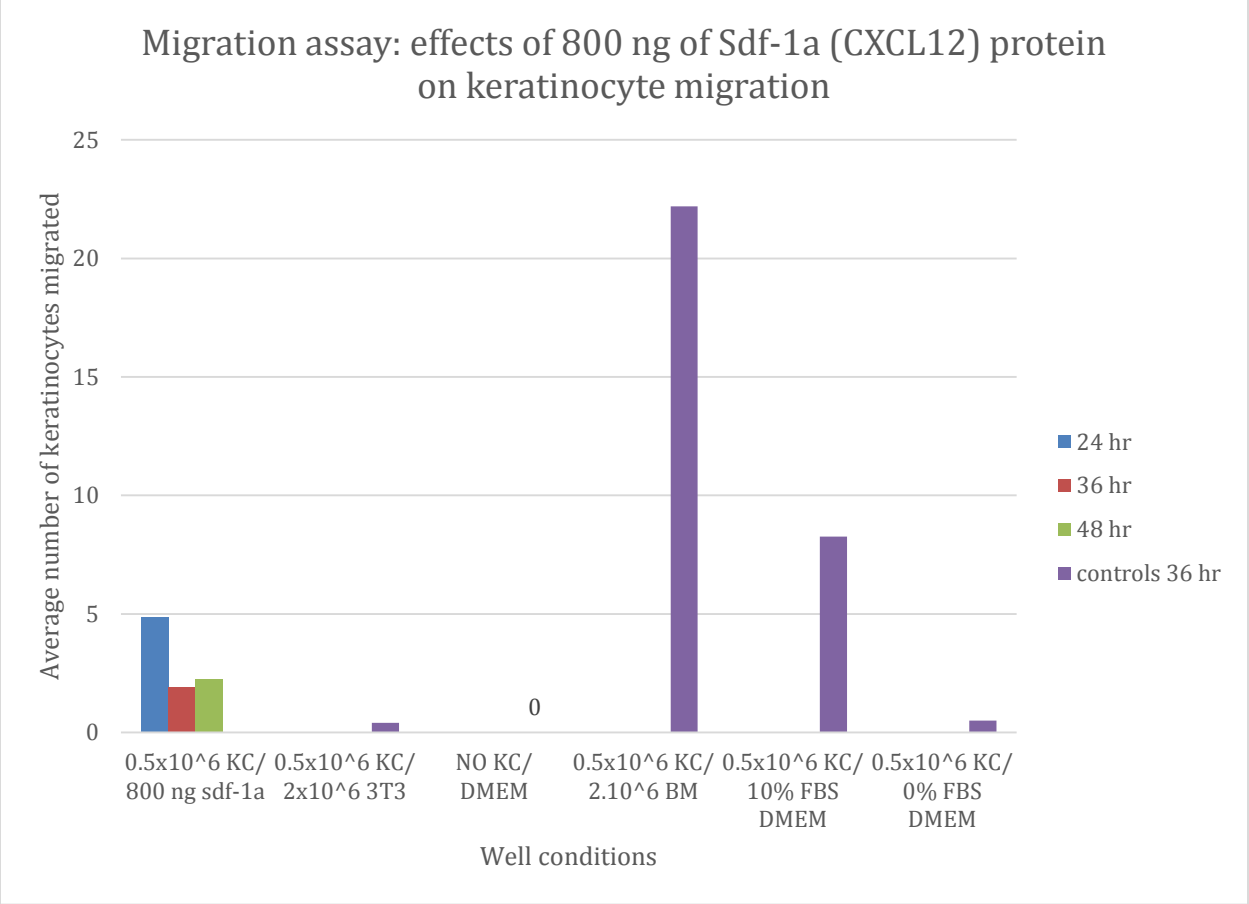

Figure 3a. CXCL12 Migration Assay Data for the first migration assay using Sdf-1a (CXCL12) as a chemoattractant was using the literature determined 800 ng as the optimal concentration is shown here. This experiment was run using the BD Biocoat matrigel migration assay with 3 wells seeded per control condition and 6 wells seeded for the experimental group. The second repetition of this assay was with a gradient of concentrations of 2000 ng, 800 ng, and 200 ng of Sdf-1a protein. These data are still being processed. The third repetition of this assay was a repeat of the first assay and is still being counted.

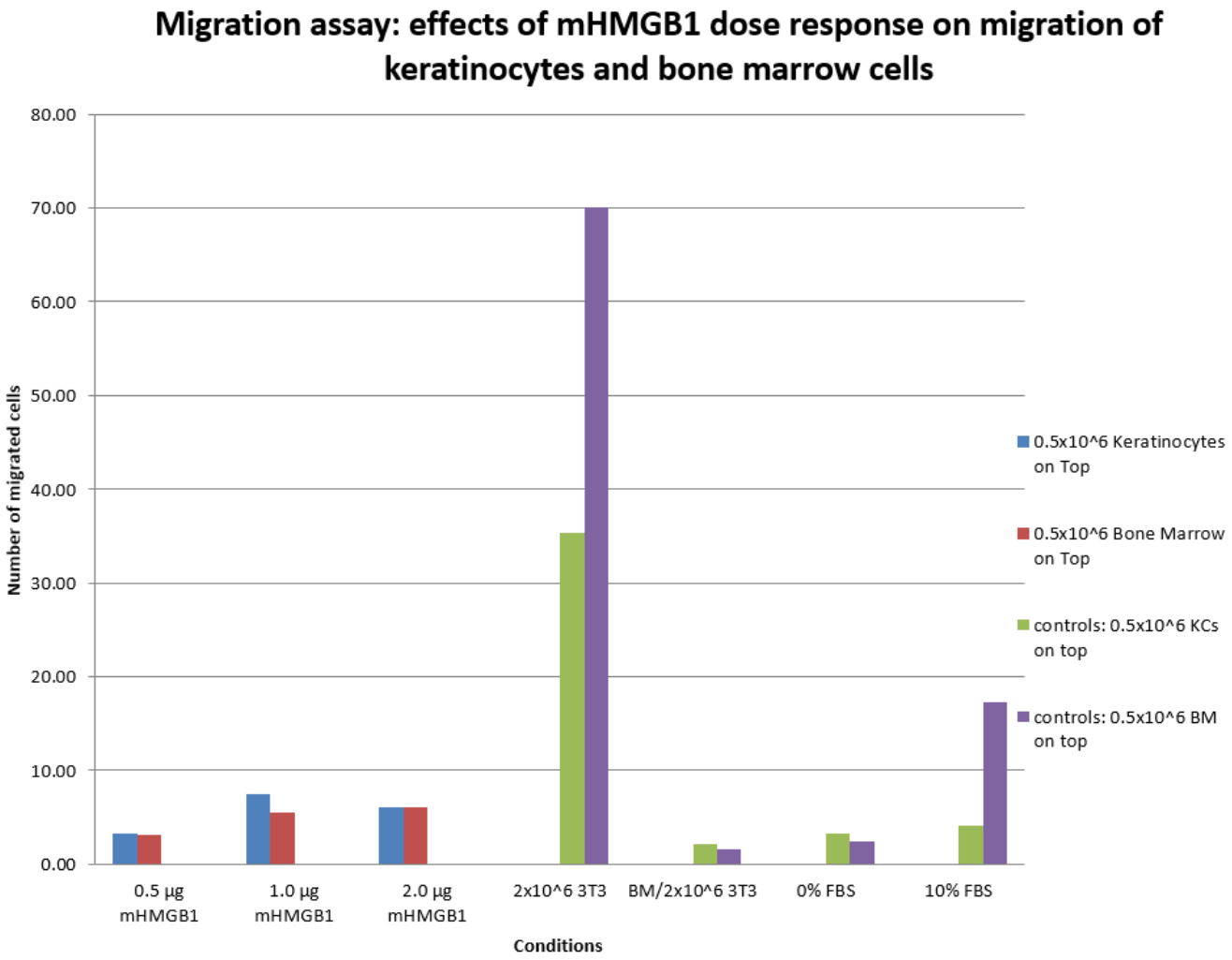

Figure 3b. HMGB1 Migration Assay First trial using mHMGB1 as chemoattractant. 3 wells were seeded for all conditions except for the 1.0 ug mHMGB1 dose in which 6 wells were seeded and all wells were run for 36 hours. We believe there was a problem with the quality of the KCs in this experiment as the KC over BM control wells have far less migration than seen in previous trials.

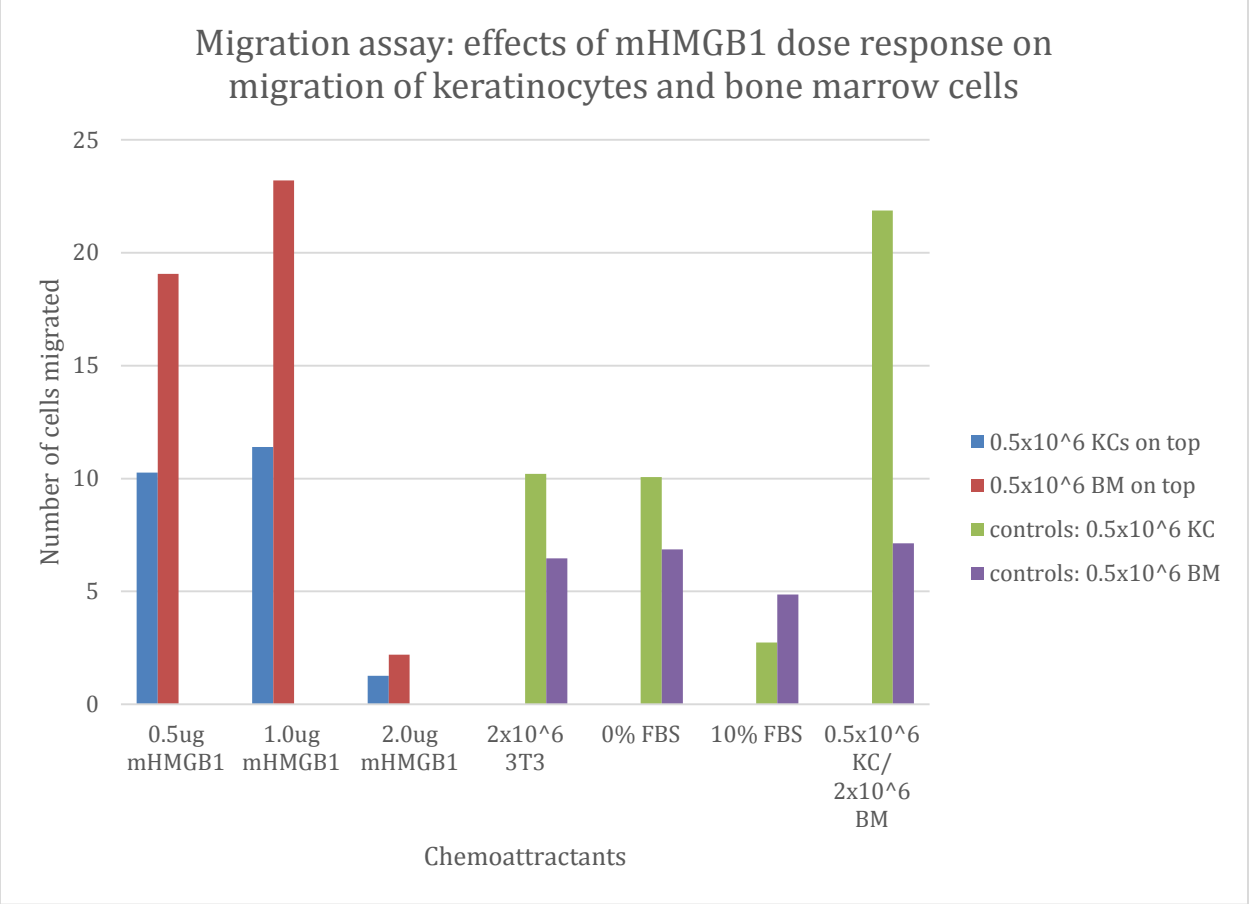

Figure 3c. Second trial using mHMGB1 as chemoattractant. 3 wells were used for all conditions except for the 1.0 ug mHMGB1 dose in which 6 wells were used. These results demonstrate that although keratinocytes are not significantly attracted to mHMGB1 as bait, the bone marrow cells are attracted to the HMGB1 as bait.

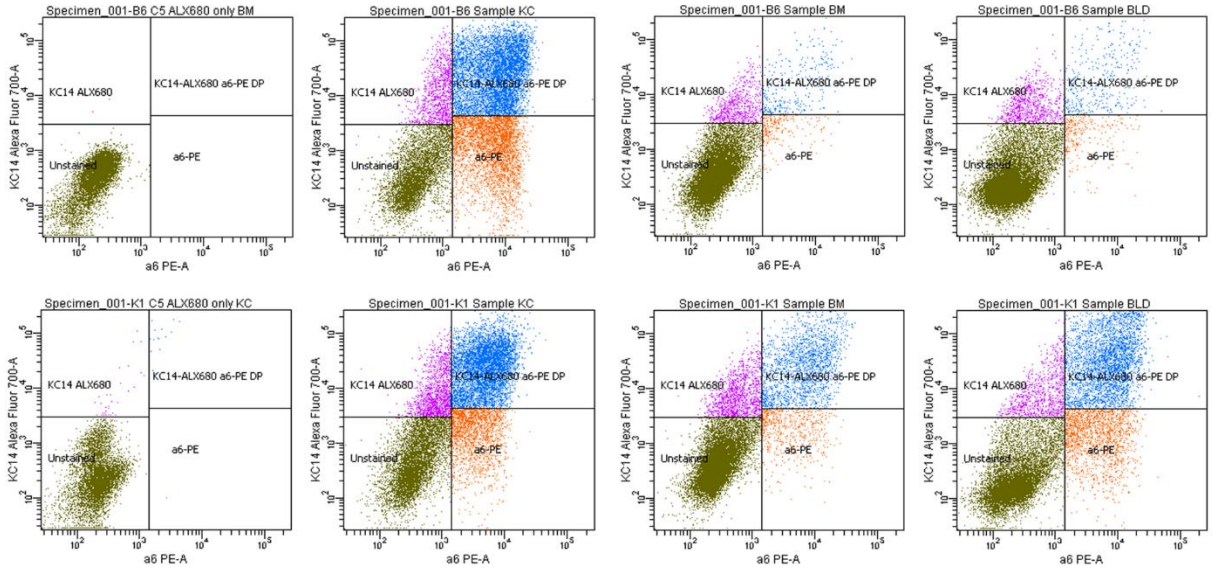

		K14-/a6-	K14+/a6-	K14+/a6+	K14-/a6+
KC	Control	31.6	6	38.1	24.3
	UV	41.6	9.3	35.7	13.7
BM	Control	93	3.9	1.7	1.5
	UV	78.7	7.1	10.5	3.6
BLD	Control	90.5	5.2	2.3	1.9
	UV	61	5.4	21.9	11.7

Figure 4a (FACS dot plot) and (table). FACS of KCs in blood and bone marrow. The percent distribution of K14 and a6 subpopulations among KCs, BM, and BLD samples in solar UV treated and control C57BL/6 mice. In BM (red boxes) and BLD (blue boxes) there is an increase in the K14+/a6+ subpopulation after UV treatment. There is also a decrease in the K14-/a6- subpopulation in BM and BLD samples and an increase in the K14-/a6+ subpopulation in only BLD samples.

Keratin 14 immunoreactive cells are found in bone marrow

Mouse Strain	Tissue Type	Treatment Duration	Treatment Type	%K14+ cells
C57BL/6	KC	0	none	+++
C57BL/6	KC	0	none	+++
C57BL/6	BM	1x	UV	++
C57BL/6	BM	1x	UV	++
SKH-1	BM	12 wk	UV	+++
C57BL/6	BM	24 wk	UV	++
C57BL/6	BM	31 wk	DMBA/TPA	++

+ Low ++ Medium +++ High

Figure 4b. Percentage of K14 in immunofluorescence microscopy (table). Mice underwent UV or chemical treatment to induce tumor formation. At different intervals of carcinogenesis bone marrow was collected, smears were made and then stained with fluorescent antibodies to keratin 14. Keratin 14 immunoreactive cells and negative nucleated cells were counted and the percentage positive calculated. This table shows that keratin 14 is seen not only at a greater presence than most of the keratinocytes as expected in untreated mice, but that at a middle time point of 12 weeks of UV treatment from an SKH-1 mouse with papilloma development there is also a high incidence of keratin 14 in the bone marrow. These results confirm the FACS results in figure 4a that keratin 14 immunoreactive cells are found in the bone marrow both before and during cutaneous carcinogenesis.

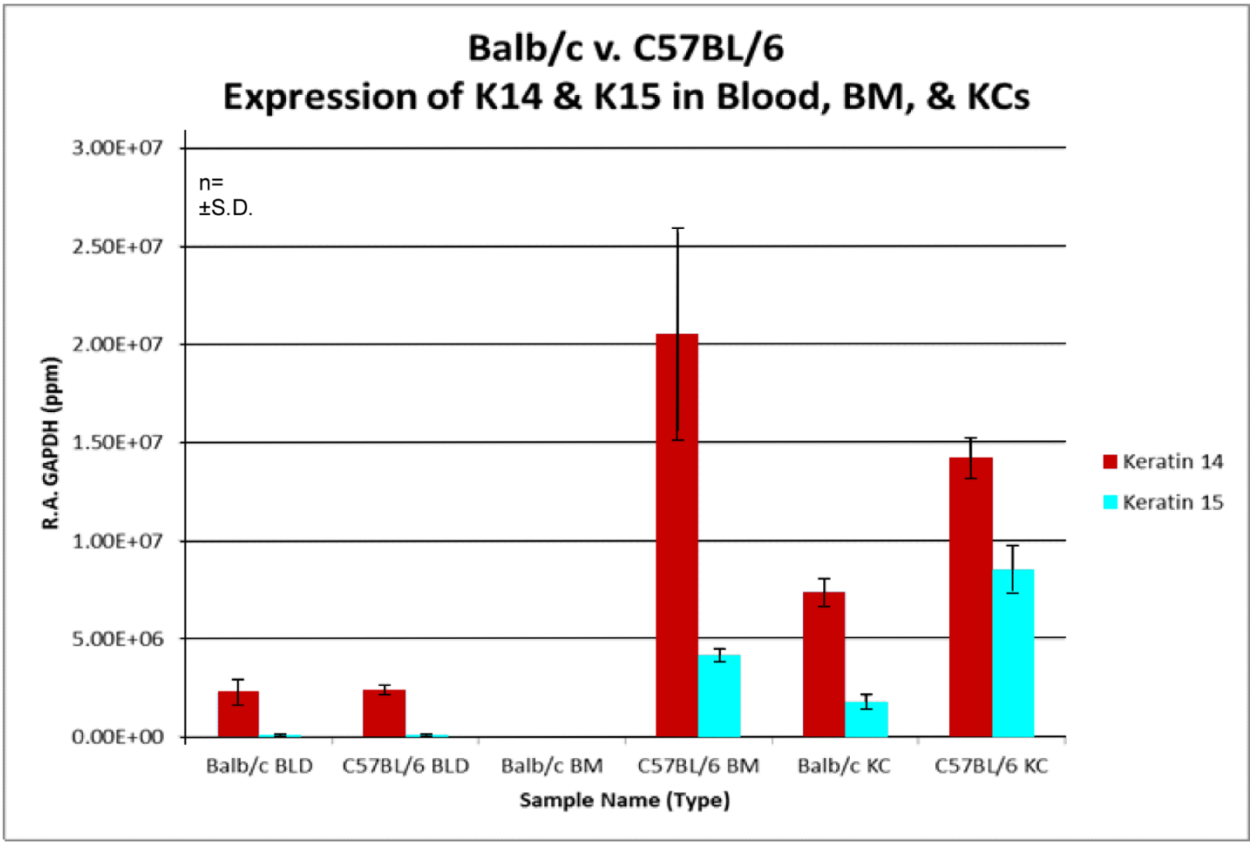

Figure 4c. QPCR for KCs in blood and bone marrow of normal, untreated mice. This graph is the compiled data from 3 replicate assays in which each assay had triplicate wells for each condition. Keratin 14 and 15 expression in the blood and bone marrow of BALB/c and c57BL/6 mice in terms of relative abundance. Keratin 14 is known to be present in all basal keratinocytes whereas keratin 15 is present in the CD49f+/CD34+ hair follicle stem cells. The surprising thing we see here is that keratin 14 is expressed in both blood and bone marrow of C57BL/6 mice and in blood of BALB/c mice. We were also surprised to detect keratin 15 in the bone marrow of C57BL/6 mice.

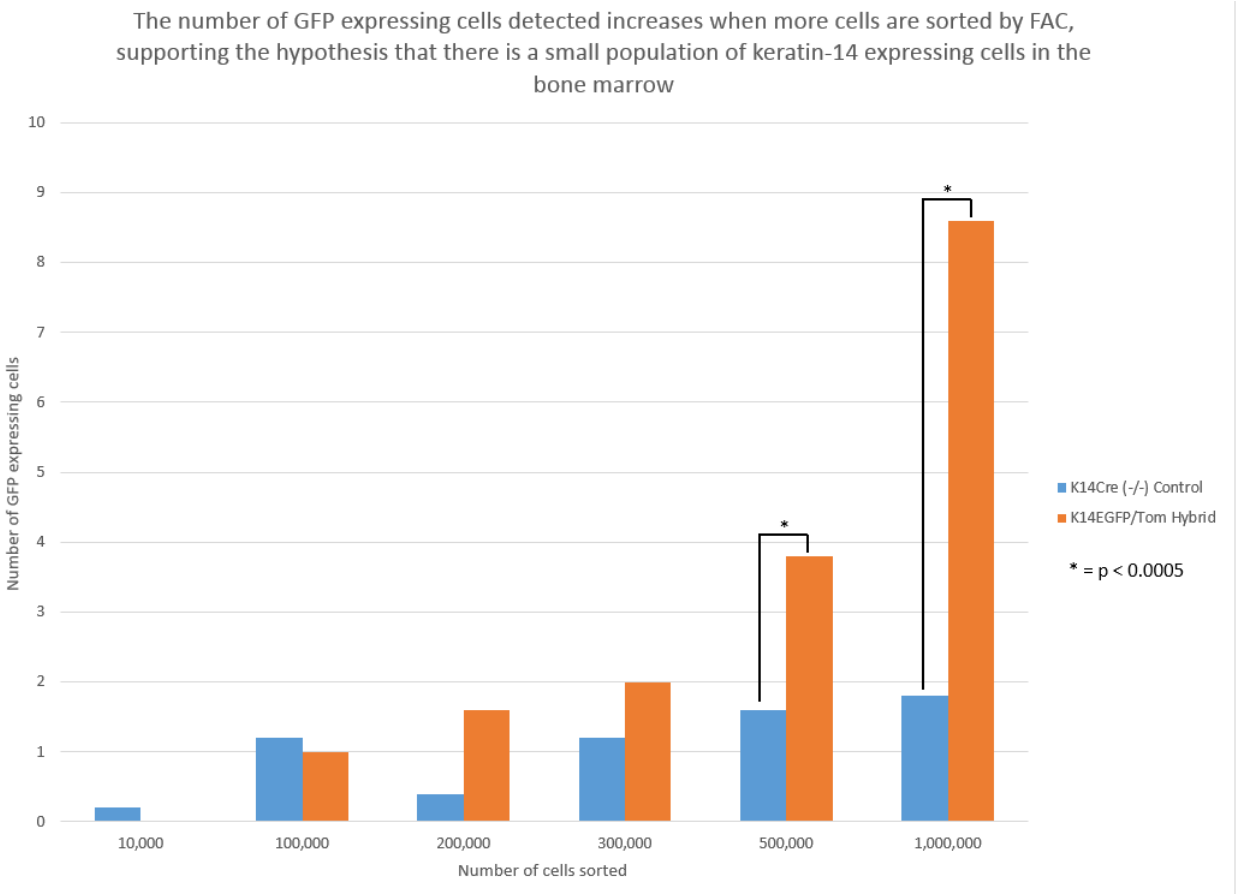

Figure 5. Fluorescent activated cell sorting (FACS) shows increased detection of GFP expressing keratin-14 cells in the bone marrow as more cells are sorted. In the K14-EGFP-Tom mice, K14 expressing cells naturally fluoresce “green” whereas all other cells naturally fluoresce “red”. The average number of K14-EGFP fluorescent labeled cells in the bone marrow of K14-EGFP-Tom hybrid increased as a larger number of cells were sorted in a sample. A two-tailed T-test shows statistical significance ($p < 0.0005$) between the K14-EGFP-Tom cells and the negative control cells when 500,000 or 1,000,000 cells are sorted.

Table 1: Inconclusive results regarding the migration of keratin 14 GFP expressing cells found in the blood of SCID mice after receiving keratinocyte skin grafts. The GFP positive signal detected from FACS is mostly part of a tail that has believed to be due to damaged cells

Ms #	Treatment	Date Euth	# cells	% Double Negative	% GFP	% TomRed	% Double Positive
3	SCID-K14Cre	1d	100,000	100	0	0	0
			500,000	100	0	0	0
			700,000	100	0	0	0
5	SCID-K14Cre	4d	100,000	100	0	0	0
			500,000	100	0	0	0
			1,000,000				
6	SCID-K14Cre	4d	100,000	100	0	0	0
			500,000	100	0	0	0
			1,000,000				
1	SCID-K14Cre	7d	100,000	100	0	0	0
			500,000	100	0	0	0
			1,000,000				
4	SCID-K14Cre	7d	100,000	99.9	0.1	0	0
			500,000	99.9	0.1	0	0
			1,000,000				
2	SCID-K14Cre	7d	100,000	99.2	0.8	0	0
			500,000	99.2	0.8	0	0
			1,000,000				
7	SCID-K14Cre	14d	100,000	100	0	0	0
			500,000	100	0	0	0
			1,000,000				
8	SCID-K14Cre	14d	100,000	100	0	0	0
			500,000	100	0	0	0
			1,000,000				
10	SCID-K14GFP	4d	100,000	100	0	0	0
			500,000				
			1,000,000				
11	SCID-K14GFP	4d	100,000	100	0	0	0
			500,000	100	0	0	0
			1,000,000				
12	SCID-K14GFP	7d	100,000	99.3	0.7	0	0
			500,000				
			1,000,000				
13	SCID-K14GFP	7d	100,000	99.1	0.9	0	0
			500,000	99	1	0	0
			1,000,000				
14	SCID-K14GFP	14d	100,000	100	0	0	0
			500,000	100	0	0	0
			700,000				
15	SCID-K14GFP	14d	100,000	99.5	0.5	0	0
			500,000				

			1,000,000				
	UBC-GFP	4d	100,000	8	92	0	0
			500,000	7.9	92.1	0	0
			1,000,000				
	ROSA-TOM	4d	100,000	99.9	0.1	0	0
			500,000				
			1,000,000				
	UBC-GFP	7d	100,000	5.6	94.4	0	0
			500,000				
			1,000,000				
	ROSA-TOM	7d	100,000				
			500,000	17.9	0	82.1	0
			1,000,000				
	UBC-GFP	14d	100,000	11.1	0	88.9	0
			500,000				
			1,000,000				
	ROSA-TOM	14d	100,000	17.5	0	82.5	0
			500,000				
			1,000,000				
	Neg	14d	100,000	100	0	0	0
			500,000				
			1,000,000				

Table 2: No migration of keratin 14 GFP expressing cells in the bone marrow of SCID mice after receiving keratinocyte skin grafts.

Ms #	Treatment	Date Euth	# cells	% Double Negative	% GFP	% TomRed	% Double Positive
3	SCID-K14Cre	1d	100,000	100	0	0	0
			500,000	100	0	0	0
			700,000	100	0	0	0
5	SCID-K14Cre	4d	100,000	100	0	0	0
			500,000	100	0	0	0
			1,000,000	100	0	0	0
6	SCID-K14Cre	4d	100,000	100	0	0	0
			500,000	100	0	0	0
			1,000,000	100	0	0	0
1	SCID-K14Cre	7d	100,000	100	0	0	0
			500,000	100	0	0	0
			1,000,000	100	0	0	0
4	SCID-K14Cre	7d	100,000	100	0	0	0
			500,000	100	0	0	0
			1,000,000	100	0	0	0
2	SCID-K14Cre	7d	100,000	100	0	0	0
			500,000	100	0	0	0
			1,000,000				
7	SCID-K14Cre	14d	100,000	100	0	0	0
			500,000	100	0	0	0

			1,000,000	100	0	0	0
8	SCID-K14Cre	14d	100,000	100	0	0	0
			500,000	100	0	0	0
			1,000,000	100	0	0	0
10	SCID-K14GFP	4d	100,000	100	0	0	0
			500,000	100	0	0	0
			1,000,000	100	0	0	0
11	SCID-K14GFP	4d	100,000	100	0	0	0
			500,000	100	0	0	0
			1,000,000	100	0	0	0
12	SCID-K14GFP	7d	100,000	100	0	0	0
			500,000	100	0	0	0
			700,000	100	0	0	0
13	SCID-K14GFP	7d	100,000	100	0	0	0
			500,000	100	0	0	0
			1,000,000	100	0	0	0
14	SCID-K14GFP	14d	100,000	100	0	0	0
			500,000	100	0	0	0
			1,000,000	100	0	0	0
15	SCID-K14GFP	14d	100,000	100	0	0	0
			500,000	100	0	0	0
			1,000,000	100	0	0	0
	UBC-GFP	4d	100,000	8.1	91.9	0	0
			500,000	7.7	92.3	0	0
			1,000,000	7.2	92.8	0	0
	ROSA-TOM	4d	100,000	100	0	0	0
			500,000				
			1,000,000				
	UBC-GFP	7d	100,000	18.6	81.4	0	0
			500,000				
			1,000,000				
	ROSA-TOM	7d	100,000	16.7	0	83.3	0
			500,000				
			1,000,000				
	UBC-GFP	14d	100,000	19.5	0	80.5	0
			500,000				
			1,000,000				
	ROSA-TOM	14d	100,000	9.8	0	90.2	0
			500,000				
			1,000,000				
	Neg	14d	100,000	100	0	0	0
			500,000				
			1,000,000				

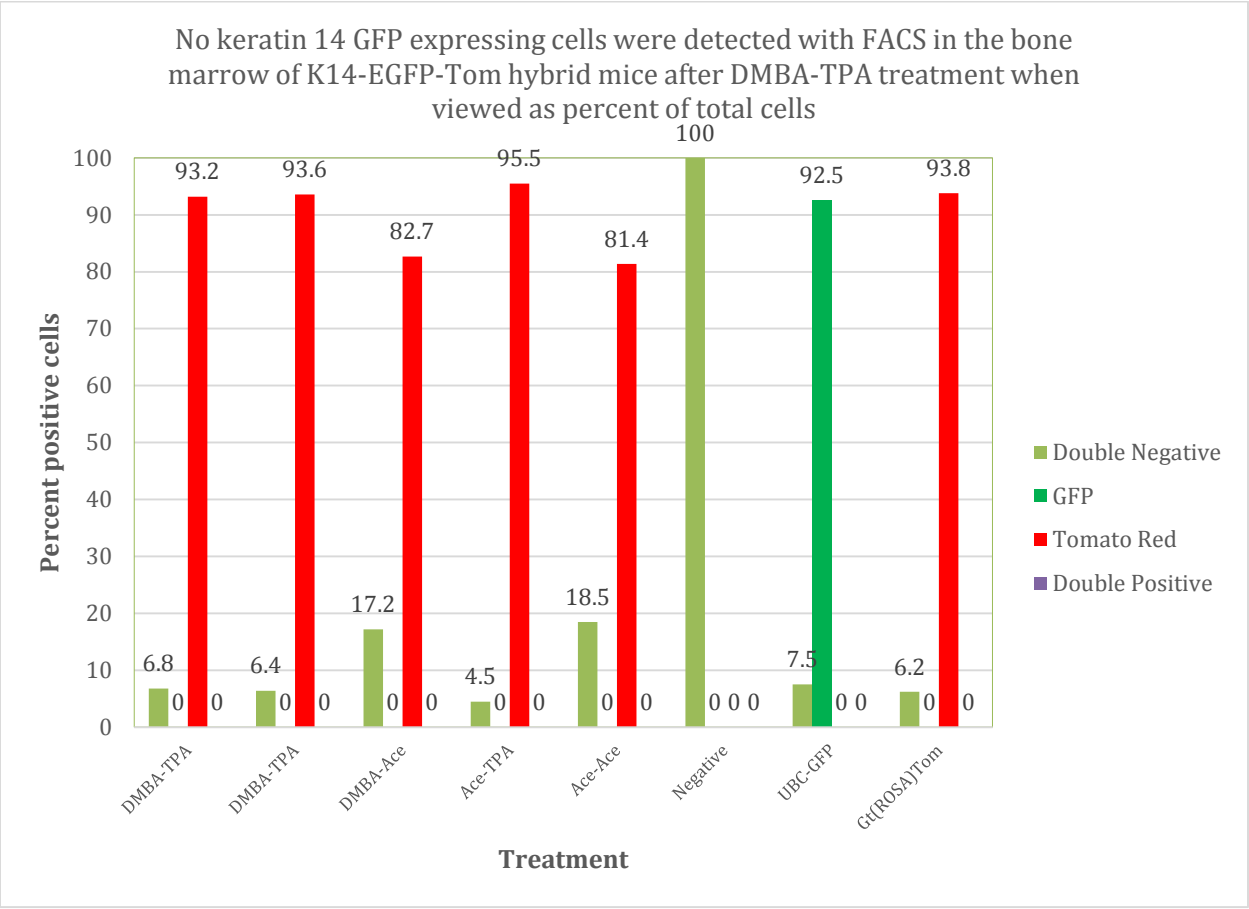

Figure 6. Fluorescent activated cell sorting (FACS) shows no K14-GFP expressing cells in the bone marrow of K14-EGFP-Tom hybrid mice after receiving DMBA and TPA treatment. The percent distribution of K14-EGFP fluorescent labeled cells in the bone marrow of K14-EGFP-Tom hybrid mice after 1x initiation with DMBA and 6x promotion treatments with TPA. Acetone (Ace) was used as a control. DMBA and TPA treatments were also performed on K14Cre and B6 mice as negative controls (data omitted). No treatment was performed on the Negative, UBC-GFP, or Gt(ROSA)Tom mice as these were only used as FACS controls. In the K14-EGFP-Tom mice, K14 expressing cells naturally fluoresce “green” whereas all other cells naturally fluoresce “red”. When analyzing the bone marrow samples by percent positive cells, there are no K14 “green” cells among any of the conditions.

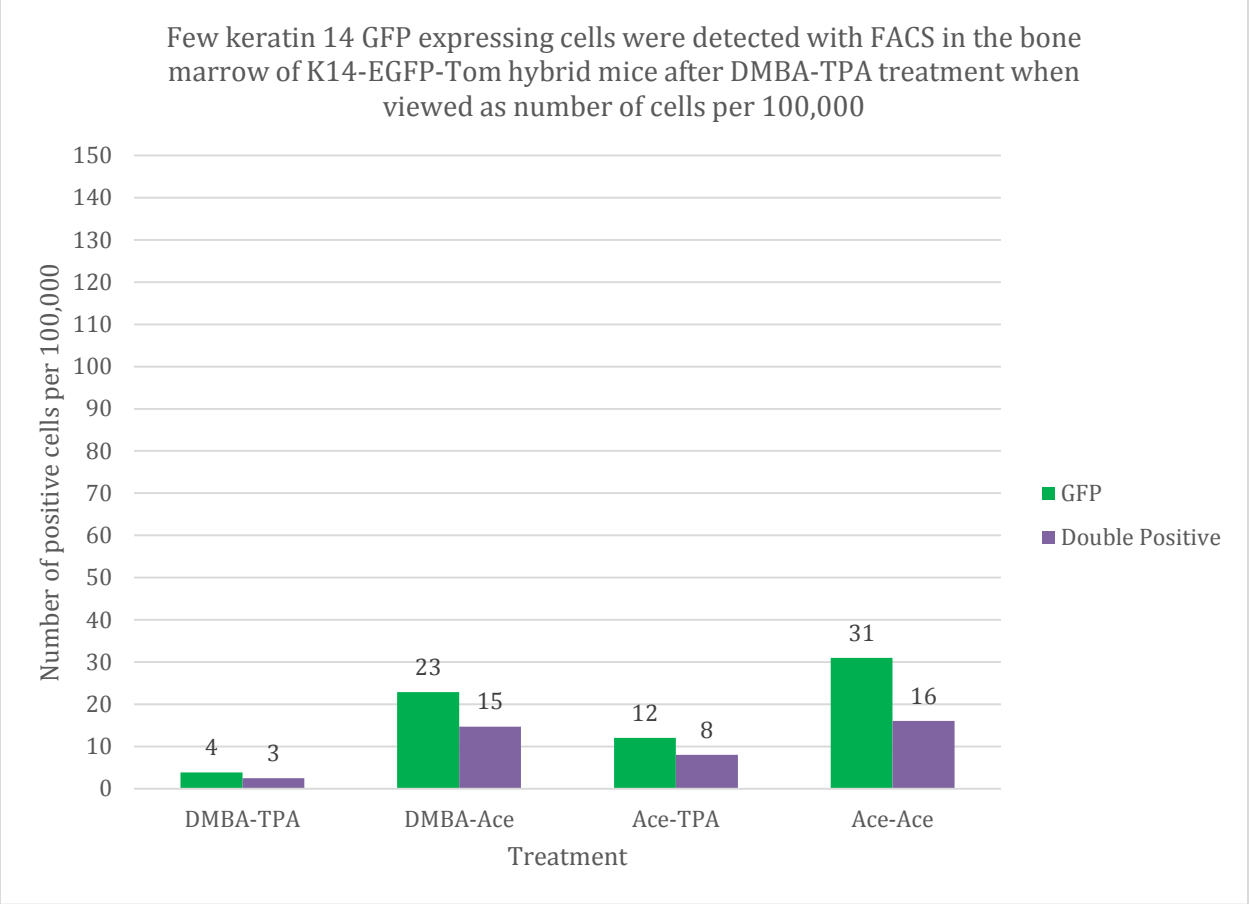

Figure 7. Fluorescent activated cell sorting (FACS) shows slight detection of K14-GFP expressing cells in the bone marrow of K14-EGFP-Tom hybrid mice after receiving DMBA and TPA treatment cells. The number of positive K14-EGFP fluorescent labeled cells per 100,000 sorted in the bone marrow of K14-EGFP-Tom hybrid mice after 1x initiation with DMBA and 6x promotion treatments with TPA. Acetone (Ace) was used as a control. DMBA and TPA treatments were also performed on K14Cre and B6 mice as negative controls (data omitted). In the K14-EGFP-Tom mice, K14 expressing cells naturally fluoresce “green” whereas all other cells naturally fluoresce “red”. When analyzing the bone marrow samples by number of GFP positive or GFP/TomatoRed double positive cells, there are fewer GFP positive and GFP/TomatoRed double positive cells in the DMBA-TPA treatment groups than in the various controls.

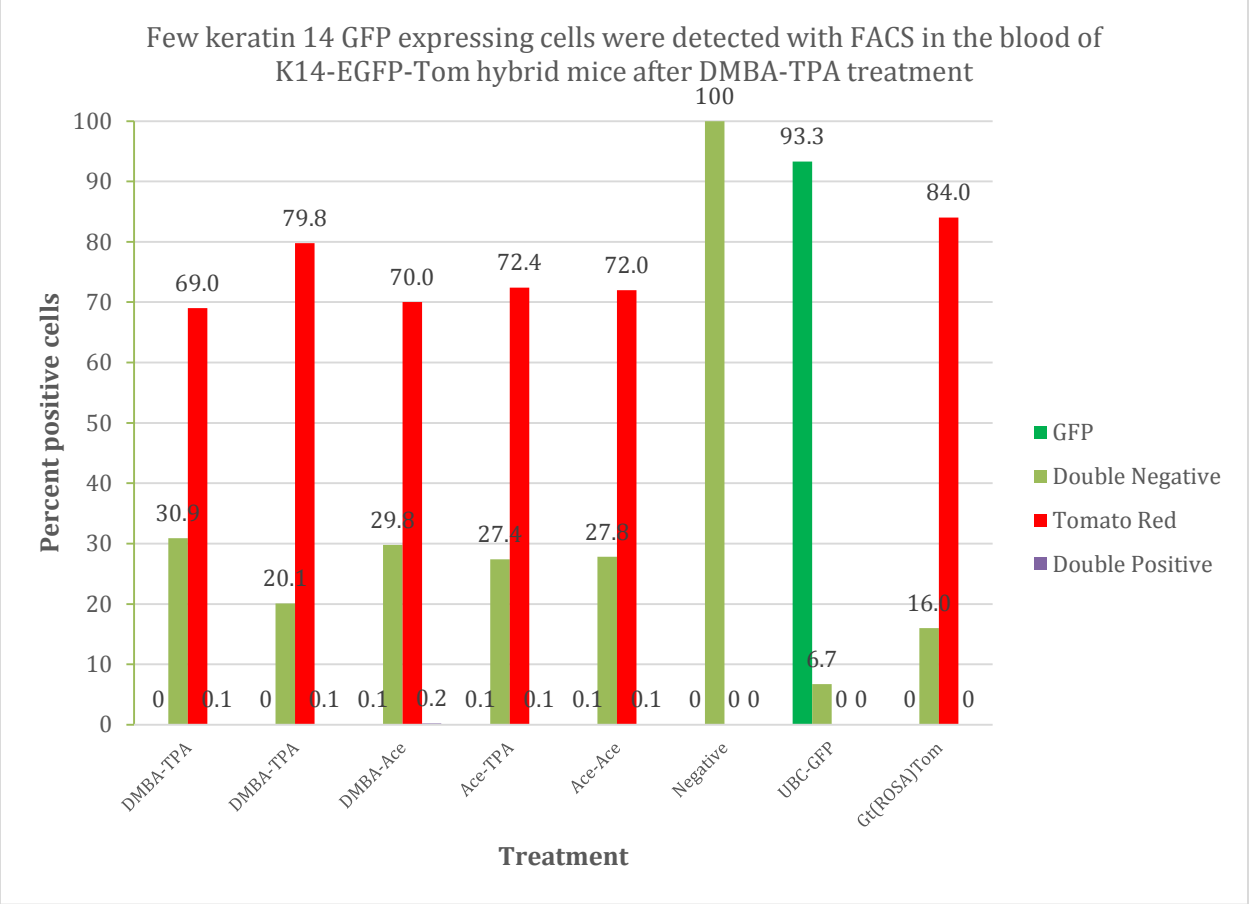

Figure 8. Fluorescent activated cell sorting (FACS) shows slight detection of K14-GFP expressing cells in the blood of K14-EGFP-Tom hybrid mice after receiving DMBA and TPA treatment (data displayed as 0-100% total cells). The percent distribution of K14-EGFP fluorescent labeled cells in the blood of K14-EGFP-Tom hybrid mice after 1x initiation with DMBA and 6x promotion treatments with TPA. Acetone (Ace) was used as a control. DMBA and TPA treatments were also performed on K14Cre and B6 mice as negative controls (data omitted). No treatment was performed on the Negative, UBC-GFP, or Gt(ROSA)Tom mice as these were only used as FACS controls. In the K14-EGFP-Tom mice, K14 expressing cells naturally fluoresce “green” whereas all other cells naturally fluoresce “red”. When analyzing the blood samples by percent positive cells, 0.1% of cells are GFP positive or GFP/TomatoRed double positive except for the DMBA-TPA treated mice in which no cells were GFP positive.

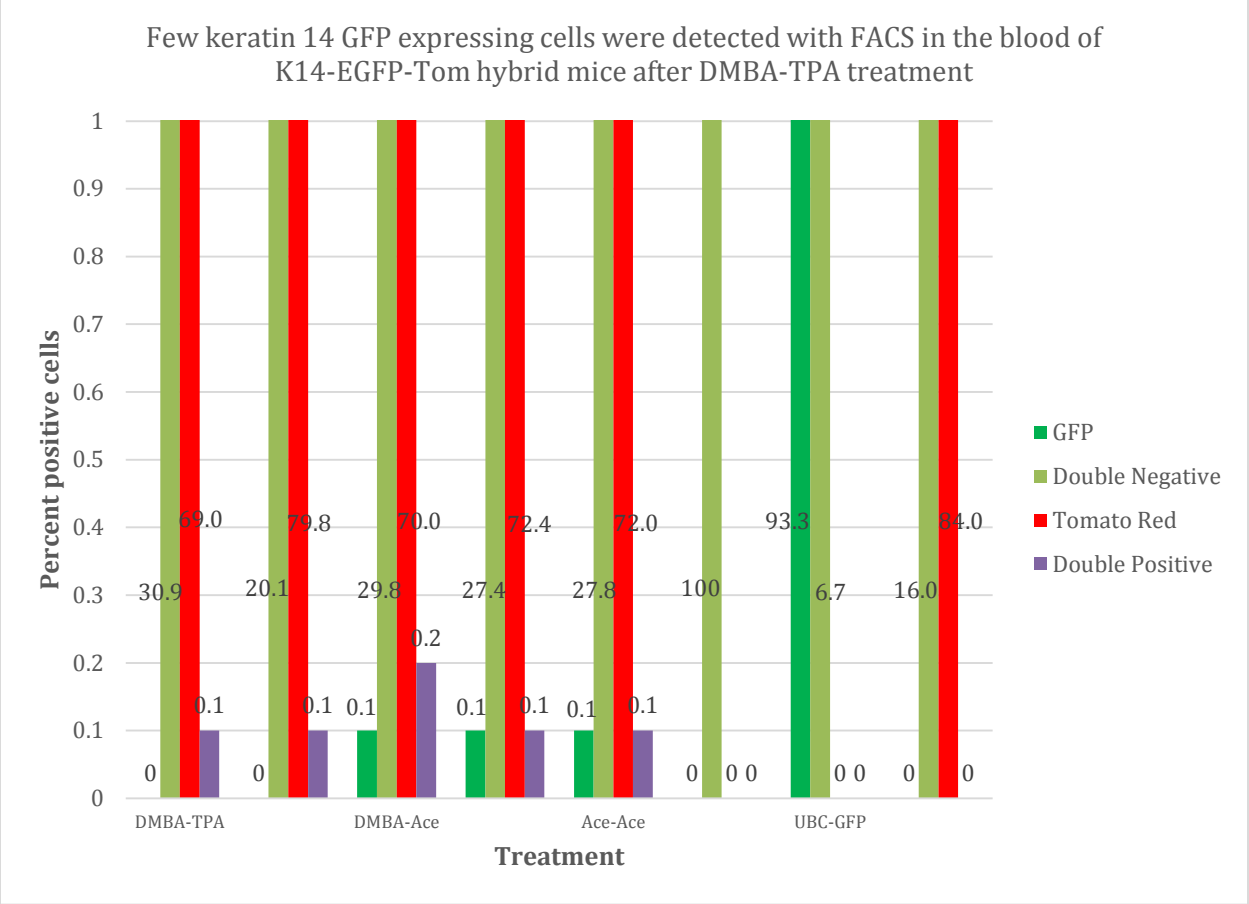

Figure 9. Fluorescent activated cell sorting (FACS) shows no K14-GFP expressing cells and slight expression of GFP/TomatoRed double positive cells in the blood of K14-EGFP-Tom hybrid mice after receiving DMBA and TPA treatment (data displayed as 0-1% of total cells). The percent distribution of K14-EGFP fluorescent labeled cells in the blood of K14-EGFP-Tom hybrid mice after 1x initiation with DMBA and 6x promotion treatments with TPA. Acetone (Ace) was used as a control. DMBA and TPA treatments were also performed on K14Cre and B6 mice as negative controls (data omitted). No treatment was performed on the Negative, UBC-GFP, or Gt(ROSA)Tom mice as these were only used as FACS controls. In the K14-EGFP-Tom mice, K14 expressing cells naturally fluoresce “green” whereas all other cells naturally fluoresce “red”. When analyzing the blood samples by percent positive cells, 0.1% of cells are GFP positive or GFP/TomatoRed double positive except for the DMBA-TPA treated mice in which no cells were GFP positive.

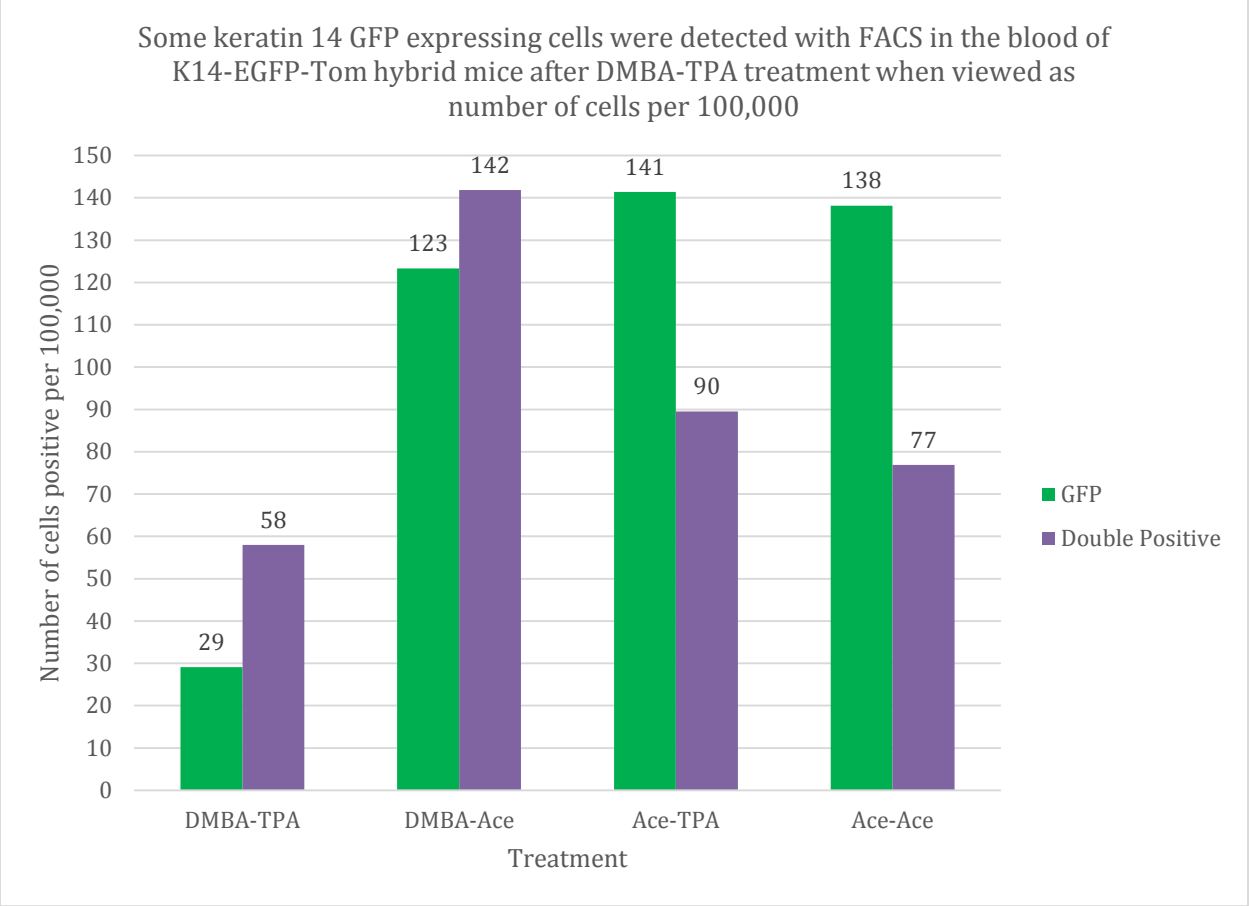

Figure 10. Fluorescent activated cell sorting (FACS) shows more K14-GFP expressing cells in the blood of K14-EGFP-Tom hybrid mice after receiving DMBA and TPA treatment than in the bone marrow. The number of positive K14-EGFP fluorescent labeled cells per 100,000 sorted in the blood of K14-EGFP-Tom hybrid mice after 1x initiation with DMBA and 6x promotion treatments with TPA. Acetone (Ace) was used as a control. DMBA and TPA treatments were also performed on K14Cre and B6 mice as negative controls (data omitted). In the K14-EGFP-Tom mice, K14 expressing cells naturally fluoresce “green” whereas all other cells naturally fluoresce “red”. When analyzing the blood samples by number of GFP positive or GFP/TomatoRed double positive cells, there are fewer GFP positive and GFP/TomatoRed double positive cells in the DMBA-TPA treatment groups than in the various controls. There are more double positive cells relative to GFP positive cells in the DMBA treatment groups than in the Acetone treatment groups.

SUPPORTING DATA:

- Figures relevant to each Task are presented as Appendix pages of this Progress Report but are described following the presentation of each Task and the Methods used to achieve it.
- There follows here a draft of a report written by a mathematician colleague, Derek Gordon, Ph.D. (Department of Genetics; Rutgers University) who provided a statistical analysis of one of our "low count" experiments. In this report, he validated our FACS data and provided support for our conclusions.

Summary – Statistical analyses of Rebecca Morris Mouse Green Fluorescent Cell Counts in Bone Marrow – Control vs. Test Mice
Date: Monday, November 30, 2015
Author: Derek Gordon

1. Testing the null hypothesis that the mean cell counts are equal in the control and test mice.

a. GFPTom-alone+ cells.

To perform this test, first we compute the mean cell counts in each group of mice (control and test). We have count data on five separate mice in each group. We determined the counts for each mouse as a function of the number of cells viewed. There were six categories of viewed cells: 10K, 100K, 200K, 300K, 500K, 1M = 1000K. We considered multiple categories to determine the minimum number of cells that need be counted to observe a sufficient number of green fluorescent cells per mouse.
We report the counts for each mouse and for each category in Table 1, as well as the *t*-test p-values where the null hypothesis of the *t*-test is that mean numbers of cells in a given category are equal for controls and tests. Regarding the *t*-test, we specify that we allow for unequal variances among the two groups; also, the p-value is a two-sided p-value.

Table 1. Green fluorescent cell counts and *t*-test p-values for control and test mice.

GFPTom-alone+ (Control)	Cell Number (Category)					
Mouse Number	10K	100K	200K	300K	500K	1M
1	0	4	1	3	1	3
2	0	2	0	2	1	2
3	0	0	0	0	0	1
4	0	0	1	0	4	2
5	0	0	0	1	2	1
Total cells in category	0	6	2	6	8	9
Mean number of cells in category	0	1.2	0.4	1.2	1.6	1.8
GFPTom-alone+ (Test)	Cell Number (Category)					
Mouse Number	10K	100K	200K	300K	500K	1M
1	0	1	2	0	1	5
2	0	1	0	4	4	7
3	0	0	2	2	4	9
4	0	2	3	1	4	11
5	0	1	1	3	6	11
Total cells in category	0	5	8	10	19	43
Mean number of cells in category	0	1	1.6	2	3.8	8.6
t-test p-value in category	NA	0.825	0.080	0.409	0.070	0.003

b. GFPTom+ and GFPTom++ cells.

We performed an additional analysis where we added the numbers of green-fluorescent and (Rosa-Tomato) red-fluorescent cells in each mouse and tested whether means where equal in control and test mouse groups. As above, we did this for 10K, 100K, 200K, 300K, 500K, and 1M cells.

We report the counts for each mouse and for each category in Table 2, as well as the *t*-test p-values where the null hypothesis of the *t*-test is that mean numbers of cells in a given category are equal for controls and tests. As above, we specify that we allow for unequal variances among the two groups and the p-value is two-sided.

Table 2. Sums of green fluorescent cell- and red fluorescent cell-counts and *t*-test p-values for control and test mice.

GFPTom+ and GFPTom++ (Control)	Cell Number (Category)					
Mouse Number	10K	100K	200K	300K	500K	1M
1	0	4	1	3	1	3
2	0	2	0	2	1	2
3	0	1	0	0	0	1
4	0	0	1	0	4	2
5	0	0	0	1	2	1
Total cells in category	0	7	2	6	8	9
Mean number of cells in category	0	1.4	0.4	1.2	1.6	1.8
GFPTom+ and GFPTom++ (Test)	Cell Number (Category)					
Mouse Number	10K	100K	200K	300K	500K	1M
1	0	1	2	3	8	12
2	0	3	2	6	8	26
3	0	0	3	8	11	21
4	0	3	7	3	8	19
5	0	1	1	6	22	24
Total cells in category	0	8	15	26	57	102
Mean number of cells in category	0	1.6	3	5.2	11.4	20.4
t-test p-value in category	NA	0.840	0.067	0.011	0.021	0.001

2. Determining significant *t*-test p-values after correction for multiple testing.

Because we performed twelve *t*-tests, we need to correct the p-values for multiple testing to what results (if any) are significant. Since the tests will be positively correlated (the data sets to which they were applied used the same bone-marrow for each mouse's six categories), we use the False Discovery Rate formula that allows for positively correlated results [1-2] .
The operative inequality is:

$$p_{(i)} \leq \frac{i \times \alpha}{N}, \qquad (1)$$

where *N* is the number of tests performed (12 based on our results in Tables 1 and 2), *i* is an index, $1 \leq i \leq N$, α is the desired family-wise error rate (0.05 in this situation), and $p_{(1)} \leq p_{(2)} \leq \cdots \leq p_{(12)}$ are the twelve p-values sorted from smallest to largest. Let I be the largest integer of 1 through 12 such that inequality (1) holds. Then the p-values $p_{(1)}, p_{(2)}, \ldots, p_{(I)}$ are all significant at the 5% level after correction for multiple testing.

Using the p-values in Tables 1 and 2 (and treating the NA values as p-values equal to 1), we determine that I =3, and the null hypothesis of equal means is rejected for the following data sets:

Table 3. Significant *t*-test p-values after correction for multiple testing.

Data Set	Cell Number	*t*-test *p*-value
GFPTom+ and GFPTom++	1M	0.001
GFPTom+	1M	0.003
GFPTom+ and GFPTom++	300K	0.011

From Table 3, we see that, when the Cell Number is one million, we observe significant difference in means of both green fluorescent and green- and red-fluorescent cell counts among controls and tests. This result suggests that we test with at least one million cells when seeking to determine count differences among control and test mice.

3. Relationship between cell number and GFPTom+ counts.

To determine the relationship between the number of cells used in an experiment and the expected number of green fluorescent cells, first we plotted the total number of green-fluorescent cells as a function the total number of cells viewed (divided by 10K) (Red line in Figure 1).

We determined the linear function by performing a regression analysis. We the method implemented the linear model method implemented in the R software package [3]. The fitted equation is: $\hat{Y} = 0.4275X$, where X is the total number of cells (divided by 10K) and $\hat{Y}$ is the predicted number of green-fluorescent cells.

As may be seen in Figure 1, the fitted equation serves as a very good approximation to the observed counts. Support for this statement is provided in the regression analysis. The *t*-test for the coefficient 0.4275 is 21.57 (p-value = 2.7E-05, 4 df). The adjusted R^2 value is 0.9893 and the F-statistic, reflecting the overall fit, is 465.3 on 1 and 4 df, with a corresponding p-value of 2.73E-05.

Conclusions

The results of these analyses suggest that, for a sufficient number of total cells in an experiment, there is a significant difference among mean control- and test-green fluorescent and green and red fluorescent cell counts, even after correction for multiple testing.

A second result is that there appears to be a linear relationship between the total number of cells counted in an experiment and the number of green-fluorescent cells. This relationship is useful, in that it helps researchers determine the minimum number of total cells necessary to detect differences among control and test populations.

Figure 1. The observed (red curve) and expected (blue curve) green fluorescent-cell counts as a function of the total number of cells per experiment (divided by 10K).

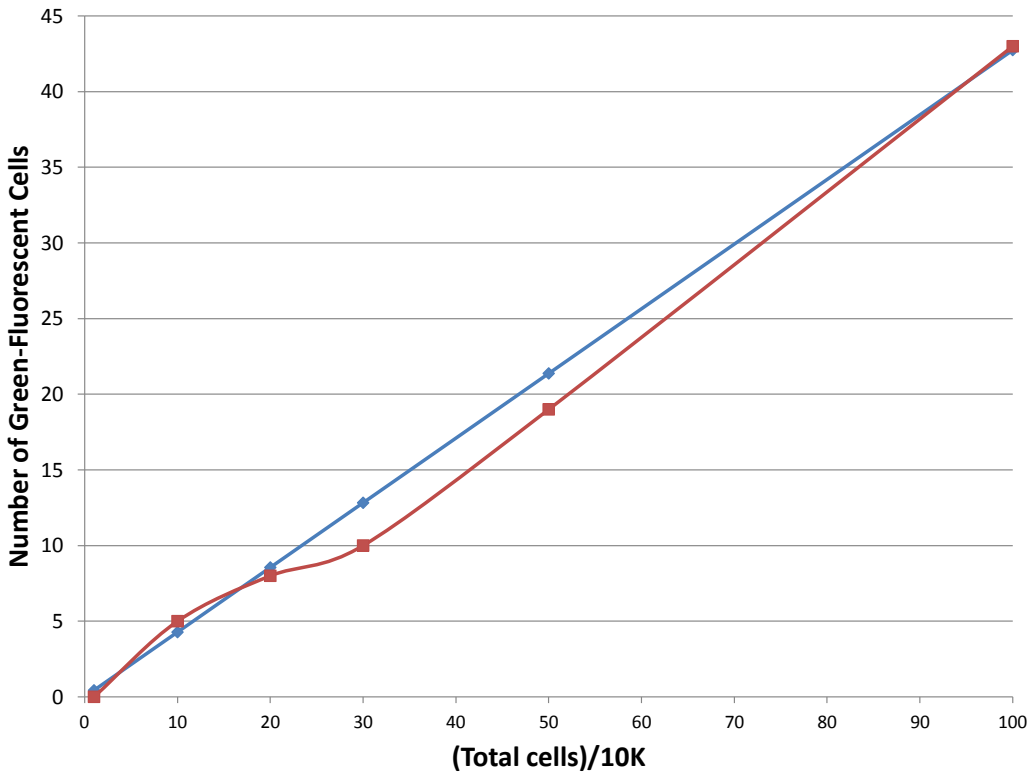

References

1 Benjamini Y, Hochberg Y: Controlling the false discovery rate: A practical and powerful approach to multiple testing. J Roy Stat Soc B 1995;57:289-300.

2 Benjamini Y, Hochberg Y: On the adaptive control of the false discovery fate in multiple testing with independent statistics. J Educ Behav Stat 2000;25:60-83.

3 R Development Core Team (2012): R: A language and environment for statistical computing. R Foundation for Statistical Computing;Vienna, Austria. ISBN 3-900051-07-0, URL http://www.R-project.org/.